# Pharmacologic activation of autophagy without direct mTOR inhibition as a therapeutic strategy for treating dry macular degeneration

Qitao Zhang[1], Feriel Presswalla[1], Robin R. Ali[1,2], David N. Zacks[1], Debra A. Thompson[1,3], Jason ML. Miller[1]

[1]Kellogg Eye Center, University of Michigan, Ann Arbor, MI 48105, USA
[2]KCL Centre for Cell and Gene Therapy, London, England WC2R 2LS, United Kingdom
[3]Department of Biological Chemistry, University of Michigan, Ann Arbor, MI 48105, USA

**Correspondence to:** Jason ML. Miller; **email:** miljason@med.umich.edu

## ABSTRACT

Dry age-related macular degeneration (AMD) is marked by the accumulation of extracellular and intracellular lipid-rich deposits within and around the retinal pigment epithelium (RPE). Inducing autophagy, a conserved, intracellular degradative pathway, is a potential treatment strategy to prevent disease by clearing these deposits. However, mTOR inhibition, the major mechanism for inducing autophagy, disrupts core RPE functions. Here, we screened autophagy inducers that do not directly inhibit mTOR for their potential as an AMD therapeutic in primary human RPE culture. Only two out of more than thirty autophagy inducers tested reliably increased autophagy flux in RPE, emphasizing that autophagy induction mechanistically differs across distinct tissues. In contrast to mTOR inhibitors, these compounds preserved RPE health, and one inducer, the FDA-approved compound flubendazole (FLBZ), reduced the secretion of apolipoprotein that contributes to extracellular deposits termed drusen. Simultaneously, FLBZ increased production of the lipid-degradation product β-hydroxybutyrate, which is used by photoreceptor cells as an energy source. FLBZ also reduced the accumulation of intracellular deposits, termed lipofuscin, and alleviated lipofuscin-induced cellular senescence and tight-junction disruption. FLBZ triggered compaction of lipofuscin-like granules into a potentially less toxic form. Thus, induction of RPE autophagy without direct mTOR inhibition is a promising therapeutic approach for dry AMD.

## INTRODUCTION

Age-related macular degeneration (AMD), the leading cause of irreversible blindness in the developed world, is marked histologically by the accumulation of lipid-rich deposits in and around the retinal pigment epithelium (RPE). Intracellular lipid-rich accumulations are termed lipofuscin while extracellular accumulations are termed drusen [1, 2]. The RPE is a polarized monolayer, facing a fenestrated capillary bed termed the choroid basolaterally and a photoreceptor cell layer apically. The RPE is a high-volume consumer of lipid via uptake of lipoprotein particles from the choroidal circulation and daily ingestion of lipid-rich outer segments (OS) from photoreceptor cells. The RPE is also a prolific lipid secretor, with lipoprotein particles directed apically providing lipid for photoreceptor OS synthesis and lipoprotein particles directed basolaterally sending unneeded lipid through Bruch's membrane to the choroid [3]. The accumulation of intracellular lipofuscin in AMD is likely the result of inefficient breakdown of phagocytosed OS [4, 5], while the accumulation of extracellular drusen likely derives from lipoprotein

particles secreted by the RPE and trapped in the underlying basement membrane [3]. Improving the RPE's capacity for lipid handling may alleviate each of these histologic hallmarks of AMD.

Autophagy is a major cellular mechanism for degrading both molecules and organelles. A *de novo* double-membrane autophagosome engulfs target cargo and then fuses with the lysosome to promote degradation of the engulfed content. Autophagy has been implicated in degradation of insoluble pathologic aggregates in neurodegenerative diseases [6] and intracellular lipid droplets in adipocytes and hepatocytes [7]. Thus, autophagy activation in the RPE may improve the clearance of insoluble lipofuscin while promoting degradation of the daily lipid load faced by RPE during OS phagocytosis and lipoprotein particle uptake. Efficient degradation of ingested lipids may, in turn, decrease secretion of drusen-inducing lipoprotein particles. Further, breakdown of fatty acids may induce ketone body (KB) production by the RPE. In turn, KB secretion by the RPE, which is almost exclusively apically directed towards photoreceptors, has been shown to provide photoreceptors with an alternate fuel source and may promote photoreceptor survival under stress [8, 9]. Thus, autophagy activation has multiple theoretical mechanisms for alleviating AMD phenotypes [10, 11].

While hundreds of small molecule and protein targets for autophagy induction have been published [12–34], we and others have previously shown that small molecule inducers of autophagy in one cell type often do not induce autophagy in other cell types [13]. Almost none of the hits from prior autophagy inducer screens have been tested for efficacy and toxicity in RPE. Further, most of the autophagy inducers tested in RPE directly inhibit mTOR or its immediate upstream kinases. Strong mTOR inhibition may disrupt RPE phagocytosis and has failed in a randomized-controlled trial for advanced dry AMD [35–37]. These data suggest methods other than direct mTOR inhibition are needed for exploring the therapeutic potential of autophagy in the RPE.

Non-primate models that replicate the features of dry macular degeneration are not available. While some genetic mouse models simulate some features of drusen, none closely recapitulate human drusen morphology and composition [38–40]. Additionally, the structure and composition of lipoprotein particles that underpin human drusen development are markedly different in mice [41]. To complement shortcomings in mouse models, primary human RPE culture models of lipoprotein secretion and drusen formation have been established [40, 42, 43].

Here, we screened small molecule activators of autophagy in primary human RPE culture that are not known to directly target mTOR or its proximal upstream kinases. One of these activators, an FDA-approved anti-helminthic called flubendazole (FLBZ), promotes degradation rather than secretion of ingested lipids, leading to production of photoreceptor-protective KBs while decreasing secretion of drusen-forming apolipoprotein. FLBZ also decreases the burden of lipofuscin accumulation while alleviating lipofuscin-induced senescence and tight-junction disruption. *In toto*, these induced changes are predicted to alleviate pathology in dry AMD.

## RESULTS

### Identifying autophagy inducers in RPE

We selected over 30 putative autophagy inducers that are not known to directly inhibit mTOR or its immediate upstream kinases and tested these inducers in a primary human fetal RPE (hfRPE) culture system [44]. Nearly all of the autophagy inducers chosen were FDA-approved compounds or have a clearly defined protein target under pharmacologic development. Previous literature suggested all compounds should induce autophagy at a low µM concentration, with the exception of fenofibrate and metformin, which have high serum concentrations at clinically relevant doses. Compounds with highly toxic mechanisms (e.g. alkylating agents) were excluded from testing, and within a pharmacologic class, no more than two compounds were tested (Table 1).

To test for autophagy induction, we measured lipidation of the core autophagy protein LC3 by mobility shift on Western blots 24 hours after each compound was added to hfRPE cultures [45]. We first confirmed that primary RPE cultures upregulate autophagy in response to classical inducers, including mTOR inhibition using the mTOR-specific inhibitor Torin1 (Torin, Figure 1A) and the upstream pan-phosphoinositide-3-kinase and mTOR dual inhibitor GSK1059615 (GSK, Figure 1A) as well as amino acid/serum starvation (Supplementary Figure 1). Of the more than 30 putative autophagy inducers tested, only five produced an increased ratio of LC3-II/LC3-I, consistent with increased autophagy (Figure 1A).

Autophagy induction was confirmed by assaying for the formation of LC3-positive puncta (autophagosomes) by immunocytochemistry [45]. Puncta formation was quantified in automated/unbiased fashion using a previously published customized macro in the Fiji/ImageJ platform [44]. Besides Torin and GSK, only two compounds, D4476, a casein kinase 1 inhibitor, and

**Table 1. Putative autophagy inducers selected for study in primary human RPE cultures.**

| Name | Abbreviation | Concentration tested in this study | Citation |
|---|---|---|---|
| GSK 1059615 | GSK | 10 μM | [46] |
| Torin1 | Torin | 1 μM | [47] |
| D4476 | | 10 μM | [20, 48] |
| Flubendazole | FLBZ | 12 μM | [12] |
| Amiodarone | | 10 μM | [49] |
| GW7647 | | 1 μM | [14] |
| JNJ-47965567 | JNJ | 10 μM | [33] |
| 2-Acetyl-5-tetrahydroxybutyl Imidazole | THI | 10 μM | [21] |
| Ac-Calpastatin | | 10 μM | [50] |
| AZ-10606120 | | 10 μM | [33] |
| Bortezomib | | 50 nM | [51] |
| BRD5631 | | 10 μM | [30] |
| Carbamazepine | | 10 μM | [52] |
| Clonidine | | 10 μM | [52] |
| Entinostat | MS-275 | 10 μM | [53, 54] |
| Erlotinib | | 10 μM | [55] |
| Fasudil | HA-1077 | 10 μM | [56] |
| Fenofibrate | | 200 μM | [57] |
| Fluphenazine | | 10 μM | [58] |
| K604 | | 10 μM | [27] |
| Loperamide | | 4 μM | [23] |
| Metformin | | 1 mM | [28] |
| ML246 | Metarrestin | 10 μM | [19] |
| Mocetinostat | | 10 μM | [53, 54] |
| Nilotinib | | 10 μM | [59] |
| Nilvadipine | | 10 μM | [60] |
| Oxaprozin | | 10 μM | [31] |
| Rilmenidine | | 10 μM | [61] |
| Saroglitazar | | 10 μM | [62, 63] |
| Sertraline | | 10 μM | [64] |
| Spermidine | | 10 μM | [26] |
| Trifluoperazine | | 1 μM | [23] |
| (±)-Verapamil | | 10 μM | [28] |

Direct mTOR inhibitors that induced autophagy in primary human fetal RPE cultures are highlighted in red. Compounds that do not directly inhibit mTOR but did induce autophagy in RPE cultures by both analysis of LC3 lipidation and LC3 puncta formation are highlighted in orange. Compounds that induced autophagy in RPE culture by only LC3 lipidation but not puncta formation are highlighted in green. All other compounds failed to induce LC3 lipidation in RPE cultures.

FLBZ, an FDA-approved anti-helminthic, also induced autophagy by this second assay (Figure 1B).

Increases in both LC3 lipidation and autophagosome formation could result from downstream blockade of autophagy at the lysosome. To confirm that our hits were genuine inducers of RPE autophagy flux, we disrupted the last step of autophagy flux, lysosomal degradation, through alkalinization of the lysosome with ammonium chloride, a well-accepted method for confirming autophagy flux [45]. As expected for elevated autophagy flux rather than downstream autophagy blockade, levels of lipidated LC3 rose for all small molecule autophagy inducers (Figure 1C) and for amino acid/serum deprivation (Supplementary Figure 1). Autophagy flux can also be demonstrated by the
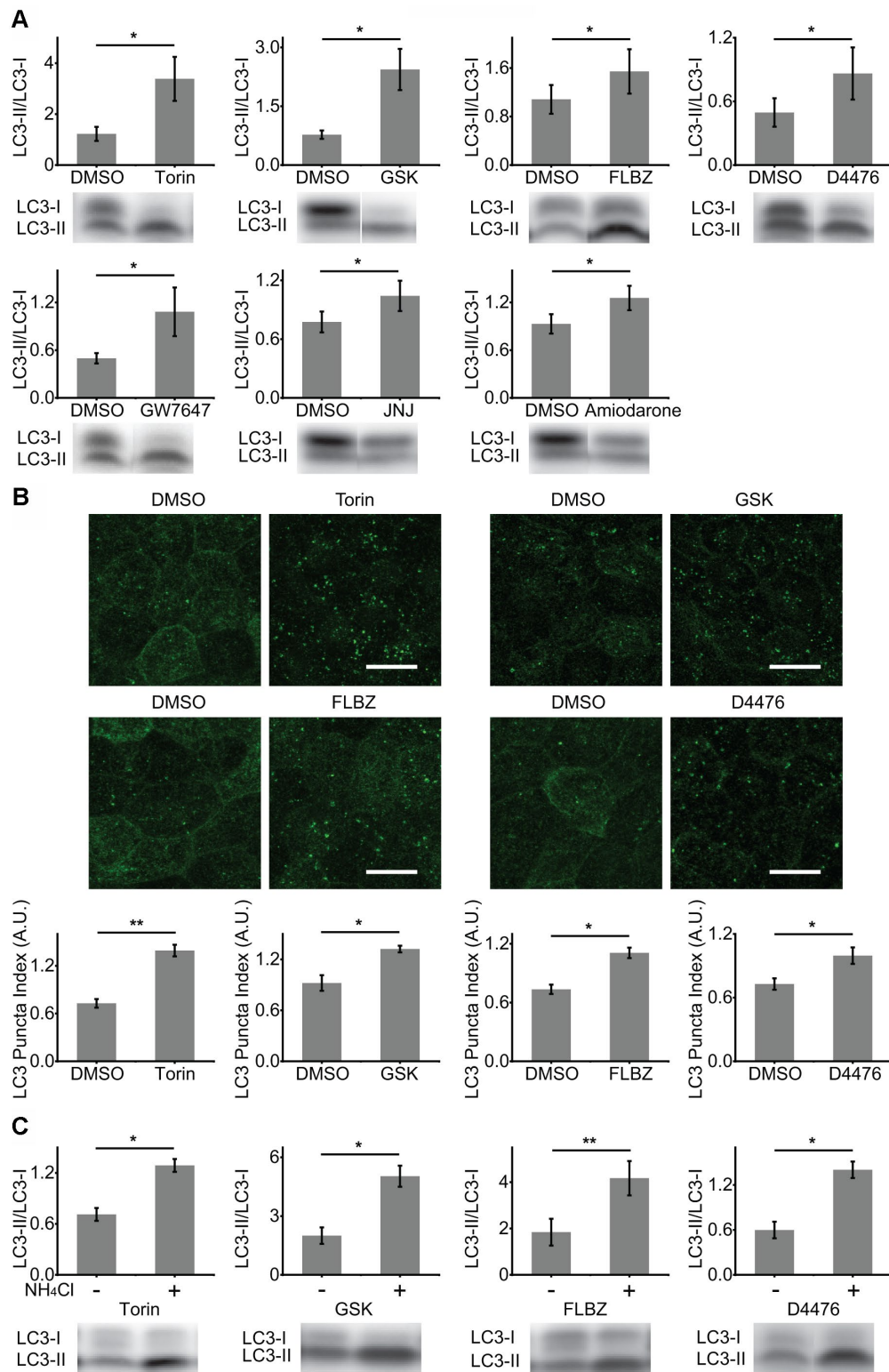
**Figure 1. Identification of autophagy inducers in primary hfRPE culture.** (**A**) Induction of autophagy by analysis of LC3 lipidation (LC3-II/LC3-I ratio). Cultures were exposed to compounds or vehicle (DMSO) for 24 hours. Torin n=8, GSK n=10, FLBZ n=10, D4476 n=8, GW7647 n=11, JNJ n=10, Amiodarone n=8. (**B**) Induction of autophagy by analysis of LC3 puncta formation (LC3 staining in green) using LC3 Puncta Index described previously [44]. Scale bar: 10 μm. Torin n=7, GSK n=3, FLBZ n=4, D4476 n=7. (**C**) Autophagy flux assays. After application of inducers or vehicle (DMSO) for 22.5 hours, 25mM of $NH_4Cl$, a lysosomal alkalizing agent, or $H_2O$ were added for a final 1.5 hours to inhibit autophagy flux. Resulting increases in the LC3-II/LC3-I ratio indicate that the compound induces autophagy flux. Torin n=6, GSK n=3, FLBZ n=6, D4476 n=5. Uncropped blots for Figure 1 in Supplementary Figure 3. *p < 0.05, **p < 0.01*.

appearance of puncta containing phosphorylated ATG16L1, which decorates newly formed autophagosomes but, unlike LC3, rapidly dissociates as the autophagosome matures [65]. Thus, the number of phospho-ATG16L1 puncta does not change with downstream blockade of autophagy. Phospho-ATG16L1 immunofluorescence confirms increased autophagy flux for both mTOR-independent autophagy inducers, FLBZ and D4476, while also demonstrating an expected decreased autophagy flux for the lysosomal poison chloroquine (Supplementary Figure 2).

**Safety of autophagy inducers**

To evaluate the safety of D4476 and FLBZ, we assessed trans-epithelial electrical resistance (TEER), a measure of tight-junction integrity, in our RPE cultures after prolonged exposure to each compound. As well-formed tight-junctions require myriad cell processes to be optimally coordinated, assessing TEER provides an easily measurable, ongoing, and non-invasive marker for general RPE cell health [66]. While both mTOR inhibitors, Torin and GSK, dramatically reduced TEER, D4476 had a more modest impact and FLBZ had no negative effect on TEER (Figure 2A). Reduced RPE pigmentation is associated with increased susceptibility to oxidative insults [67], and in contrast to cultures treated with repeated doses of FLBZ or vehicle for at least 20 days, Torin reduced RPE pigmentation (Supplementary Figure 4). Lactate dehydrogenase (LDH) release, a combined marker of necrotic and late-stage apoptotic cell death [68, 69], was reduced compared to vehicle for all four verified RPE autophagy inducers (Figure 2B). Exposure of RPE cultures to the oxidant tert-butyl hydroperoxide confirmed the ability of the assay to detect cell death (Supplementary Figure 5).

Daily OS phagocytic uptake and degradation is a core RPE function necessary for retinal function [70]. A previous study suggested that induction of autophagy in the RPE leads to impaired OS degradation after initial phagocytic internalization since autophagy and RPE phagocytosis share overlapping protein machinery [29]. While we found that autophagy induction with mTOR inhibitors did indeed impair breakdown of OS, D4476 and FLBZ had no effect on OS degradative capacity (Figure 2C).

**Effects of autophagy inducers on the balance between lipid degradation and lipid secretion**

The RPE handles an enormous lipid burden on a daily basis, including OS ingestion from its apical side and lipoprotein particle absorption from its basolateral side. Rather than storing excess lipid, the RPE may choose to degrade or secrete surplus lipids (Figure 3A). A marker of lipid degradation is the production of KBs, which are secreted by the RPE apically and serve as an energy source for photoreceptors [8, 9]. A marker of lipid secretion is the production of the apolipoprotein, apoE, which is a major component of drusen [71]. We hypothesized that autophagy inducers may promote ketogenesis through degradation of ingested lipids, reducing the stimulus for secretion of drusen-promoting apoE. In our primary RPE cultures, only FLBZ both increased production of the major KB, β-hydroxybutyrate (β-HB), and reduced the apical and basolateral secretion of apoE, suggesting that FLBZ-mediated autophagy induction changes the lipid-handling profile of RPE away from drusen promotion (Figure 3B, 3C).

**Effects of autophagy inducers on lipofuscin-like accumulation**

We have developed and extensively characterized a model of lipofuscin-like material accretion through repeated feeding of photo-oxidized OS (oxOS) to primary hfRPE culture [72]. Twenty-plus oxOS feedings over the course of a month results in a significant and stable autofluorescent granule burden (Figure 4A). With time, these granules, which we term undigestible autofluorescent material (UAM), resemble the size and emission spectrum of lipofuscin. Like lipofuscin, UAM stain with Nile Red, a marker of neutral lipids, and frequently combine with melanosomes to form melanolipofuscin granules [72].

The concurrent feeding of oxOS and FLBZ at 12μM over the course of a month resulted in significantly less UAM accumulation compared to feedings of oxOS plus vehicle (Figure 4B). Since FLBZ has no effects on phagocytosis efficiency (Figure 2C), this reduction in UAM accumulation was not due to less uptake of oxOS in the FLBZ group. We also saw LC3 colocalization with UAM granules, supporting a role of autophagy in clearing UAM (Figure 4C). Remaining UAM granules in FLBZ-treated cultures were smaller than untreated cultures (Figure 4D). In contrast, treatment with Torin at 1μM over the course of a month resulted in more UAM accumulation (Figure 4B), possibly due to inhibitory effects of Torin on phagocytic degradation (Figure 2C).

To determine whether FLBZ could reduce UAM after it had accumulated, we fed our cultures with oxOS twenty times over the course of a month, then extensively washed off OS from the cultures, and subsequently treated with twenty repeated drug feedings over the course of an additional month. FLBZ led to significantly lower levels of UAM and smaller

granule size, confirming that UAM is compactable and/or removable even after its accrual in the RPE (Figure 4B, 4D).

We and others have shown that cultures with a high UAM burden demonstrate significant senescence [72, 73], which in the RPE can contribute to the para-inflammatory state characteristic of AMD [74].

Cofeeding cultures with oxOS and FLBZ resulted in less senescence compared to feeding of oxOS plus vehicle (Figure 5A). Interestingly, when we treated cultures with FLBZ after UAM had already accumulated, cell senescence was not decreased, suggesting that established RPE senescence may be difficult to reverse (Figure 5A). Nevertheless, FLBZ still improved cell health, as assessed by tight-junction
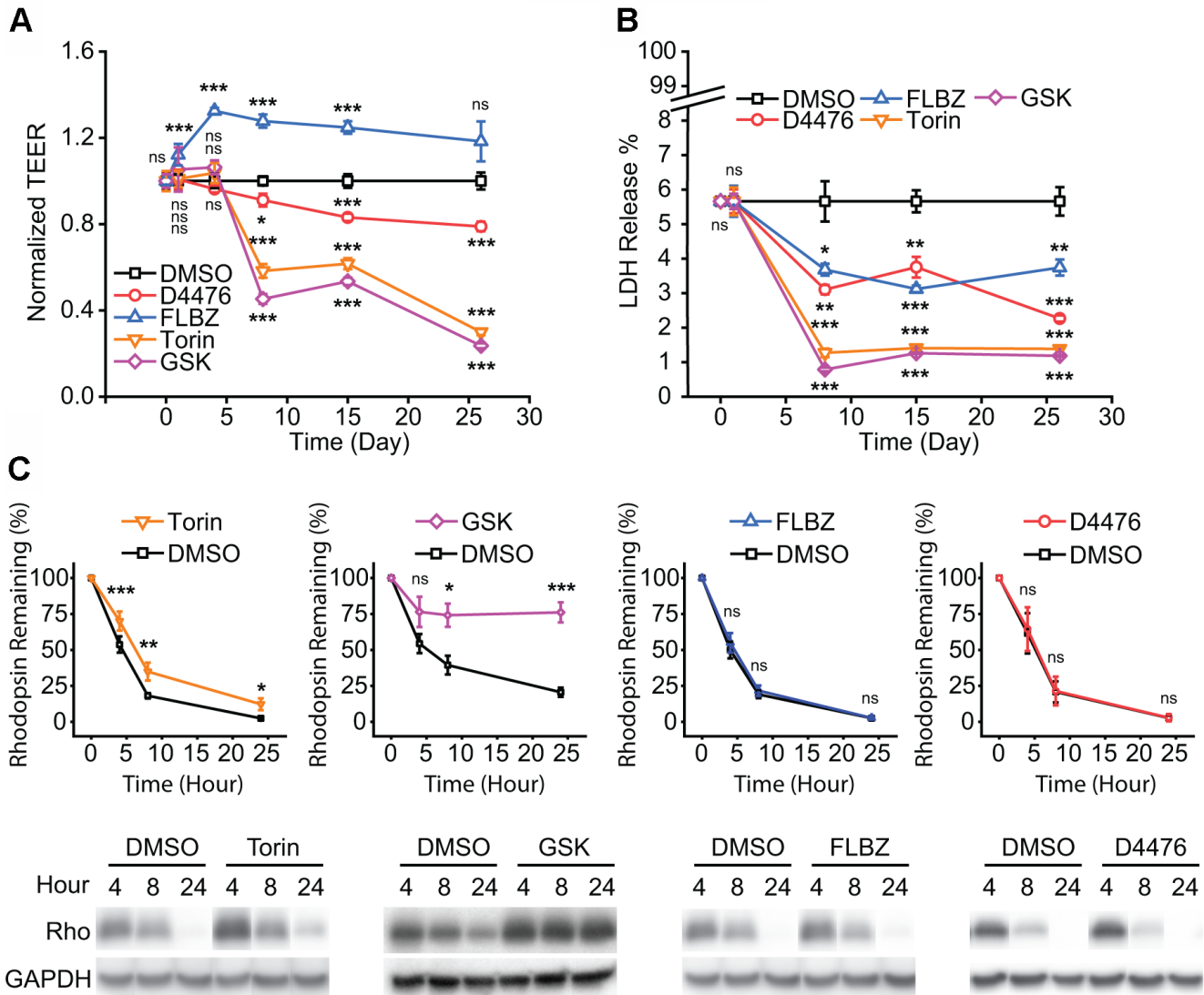


**Figure 2. Safety of confirmed autophagy inducers in primary hfRPE culture.** (**A**) Tight-junction integrity, as measured by trans-epithelial electrical resistance (TEER), is a general marker of RPE health. Drug or vehicle (DMSO) replaced daily with measurement just before drug replacement. FLBZ shows enhanced TEER while all others, especially mTOR inhibitors Torin and GSK, demonstrate progressively lower tight-junction integrity. n=6. (**B**) Cytotoxicity as measured by percent of total possible LDH release into the apical supernate. Drug or vehicle (DMSO) replaced daily with supernate collected just before drug replacement. All compounds demonstrated slightly lower cytotoxicity than DMSO control. Note scale break on Y-axis, indicating all conditions, including vehicle, demonstrated minimal LDH release. n=6. (**C**) Outer segment (OS) phagocytosis efficiency, as measured by disappearance of rhodopsin, the primary protein in OS. Purified OS are fed to RPE cultures and Western blotting for rhodopsin (Rho) indicates undigested OS remaining, as elaborated in Methods. Direct mTOR inhibition (Torin, GSK) reduces phagocytosis efficiency, whereas D4476 and FLBZ have no effect on phagocytosis. Representative blot below each graph, with GAPDH bands demonstrating equal cell mass across Transwells used for the phagocytosis assays. Torin n=12, GSK n=4, FLBZ n=9, D4476 n=3. Uncropped blots for Figure 2 in Supplementary Figure 6. *ns p > 0.05, *p < 0.05, **p < 0.01, ***p < 0.001.*

integrity, in cultures with already established UAM (Figure 5B).

## DISCUSSION

Dry AMD may be a disease of perturbed lipid homeostasis, characterized by extracellular deposition of lipid-rich drusen. The accumulation of lipid-rich intracellular lipofuscin may also be linked to AMD and Stargardt macular dystrophy [75, 76]. Efficient degradation of ingested lipid by the RPE produces KBs that are secreted and then utilized by photoreceptors for metabolism. RPE ketogenesis may promote survival of metabolically-stressed photoreceptors deprived of their primary energy source, glucose [8, 9]. For all these reasons, improving RPE lipid handling is an attractive therapeutic approach for the treatment of dry AMD.
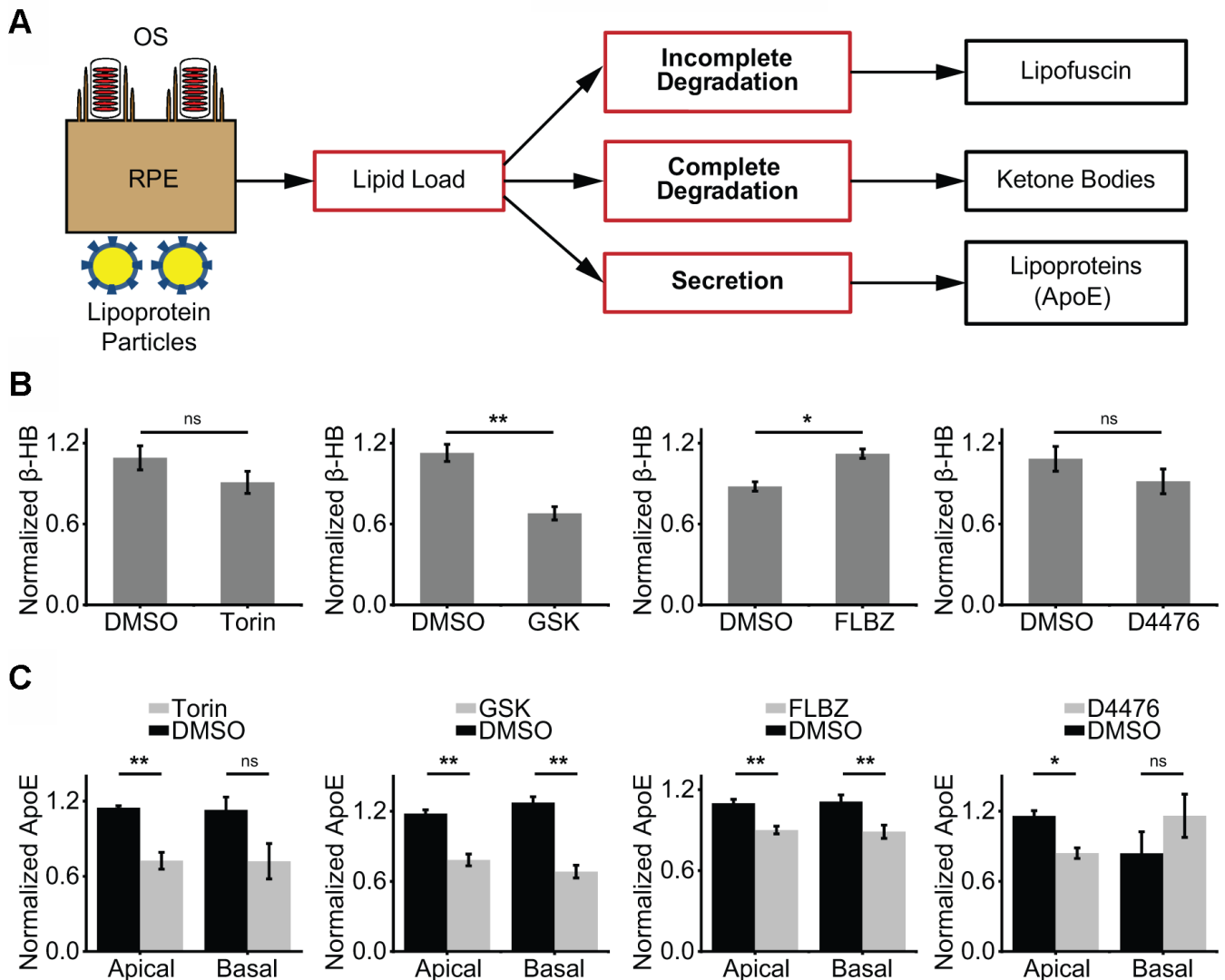


**Figure 3. Impact of confirmed autophagy inducers on RPE lipid metabolism.** (**A**) Proposed model of RPE lipid handling. Lipid-rich shed OS are phagocytosed from the apical side and lipoprotein complexes are consumed from the basolateral side daily. Incomplete lipid degradation contributes to lipofuscin accumulation. With the remaining lipid load, we postulate that the RPE daily determines the balance between complete lipid degradation, as assessed by KB production, and secretion of lipid via lipoprotein particles, as assessed by apoE secretion. (**B**) KB production (as assessed by β-hydroxybutyrate, β-HB) in the presence of vehicle (DMSO) or confirmed autophagy inducers for 24 hours. β-HB is secreted almost exclusively into the apical supernate. Only FLBZ increased lipid degradation. Torin n=4, GSK n=7, FLBZ n=6, D4476 n=4. (**C**) Apolipoprotein secretion (as assessed by apoE) in the presence of vehicle (DMSO) or confirmed autophagy inducers for 24 hours. Both apical and basolateral media contain apoE. While increasing lipid degradation in (**B**), FLBZ also decreases secretion of drusen-promoting apolipoprotein. Apical: Torin n=4, GSK n=5, FLBZ n=11, D4476 n=4. Basal: Torin n=4, GSK n=5, FLBZ n=9, D4476 n=3. *ns p > 0.05, *p < 0.05, **p < 0.01.*

Autophagy induction, which promotes lipid degradation and turnover of otherwise undigestible cellular constituents, has the potential to favorably impact RPE lipid homeostasis. However, in this study, we show that mTOR inhibition, the most common pathway for inducing autophagy, disrupts multiple RPE-specific functions. Furthermore, the mTOR inhibitor, sirolimus, failed to demonstrate therapeutic benefit in a randomized controlled trial of advanced dry AMD [37]. While researchers have pharmacologically induced autophagy in the RPE in a variety of cell and animal culture models [77–79], no explicit attempt has been made to identify lead compounds that do not directly inhibit mTOR or its immediate upstream kinases. We therefore sought to identify non-toxic autophagy inducers in primary human RPE independent of direct mTOR inhibition.

Of more than 30 putative autophagy inducers we tested, only two, D4476 and FLBZ, reliably induced autophagy in our primary human RPE cultures. Our results support prior assertions that autophagy inducers are often cell specific [13].

In evaluating autophagy inducers in the RPE, we found that mTOR inhibition disrupted RPE-specific functions,
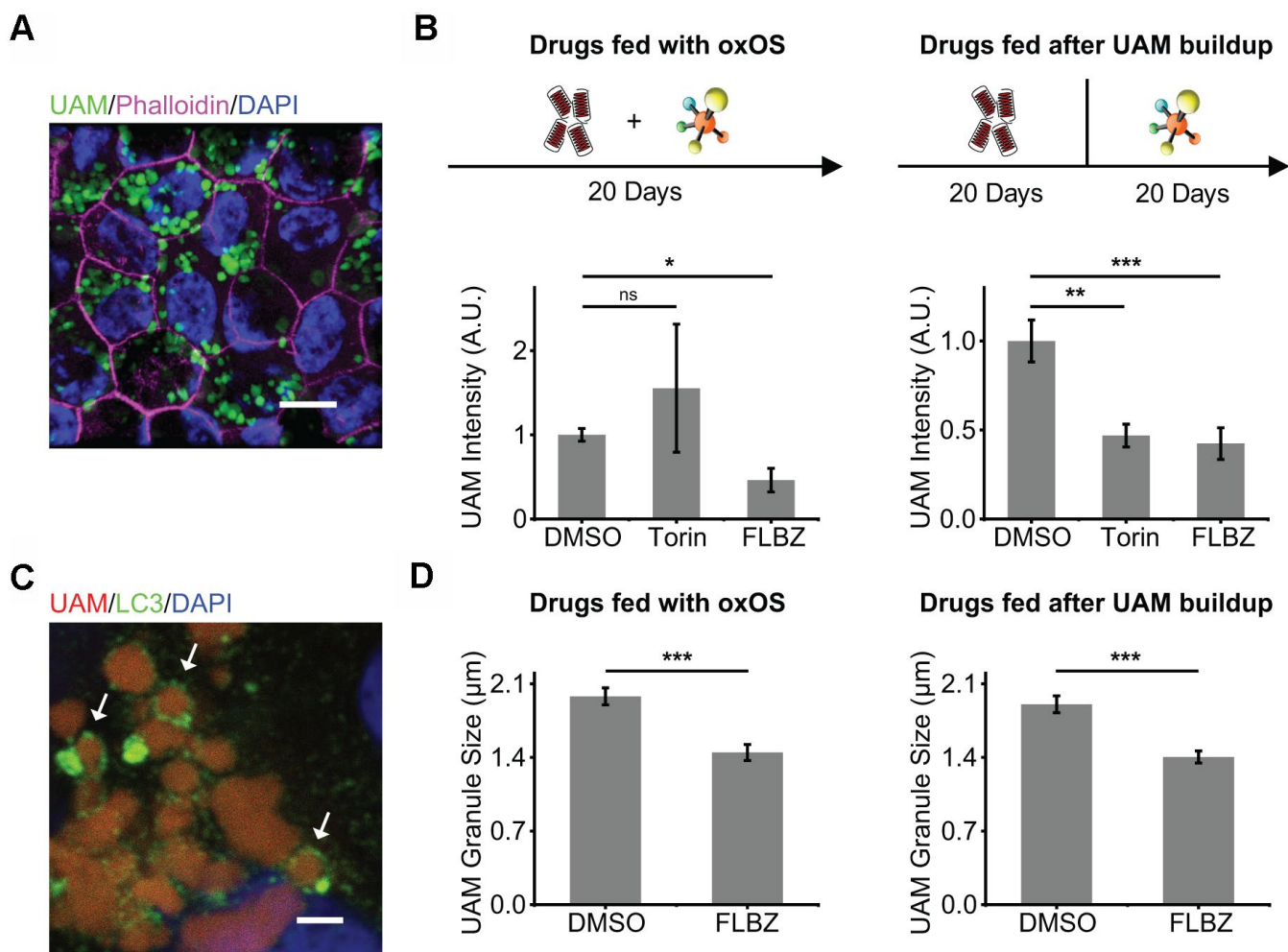


**Figure 4. Autophagy inducer FLBZ reduces accumulation of lipofuscin-like material.** (**A**) Lipofuscin-like UAM accumulates in RPE after repeated feedings of photo-oxidized outer segments (oxOS). UAM granules (green). DAPI (blue). Phalloidin stain of F-actin outlining cell borders (pink). Scale bar: 10 μm. (**B**) Effects of FLBZ or Torin on UAM accumulation (left) and elimination (right). FLBZ or Torin is fed together with oxOS daily for 20 days in a month (left, n=5) or fed daily for 20 days in a month after completion of oxOS feedings to stimulate UAM accumulation (right, n=7). Unlike Torin, FLBZ both reduces UAM accumulation and increases UAM elimination. DMSO as vehicle control. UAM normalized to DMSO condition. (**C**) LC3 colocalization to UAM granules in the human RPE cell line, ARPE-19, treated with FLBZ. UAM (red). LC3 (green). DAPI (blue). Arrows indicate LC3 puncta surrounding a lipofuscin granule. Scale bar: 2 μm. (**D**) Effects of FLBZ on UAM granule size. Compared to vehicle (DMSO), FLBZ decreases UAM granule size both during oxOS feedings (left) and after UAM buildup has already occurred (right). n=40. ns $p > 0.05$, *$p < 0.05$, **$p < 0.01$, ***$p < 0.001$.

including tight-junction integrity, OS phagocytosis, and pigmentation. The role of mTOR in RPE health is multifaceted. On the one hand, over-activation of mTOR leads to RPE dedifferentiation through an epithelial-to-mesenchymal transition [80]. mTOR activation is also associated with RPE senescence [81] and less efficient phagocytosis of OS [82]. On the other hand, timely activation of mTOR and upstream kinases
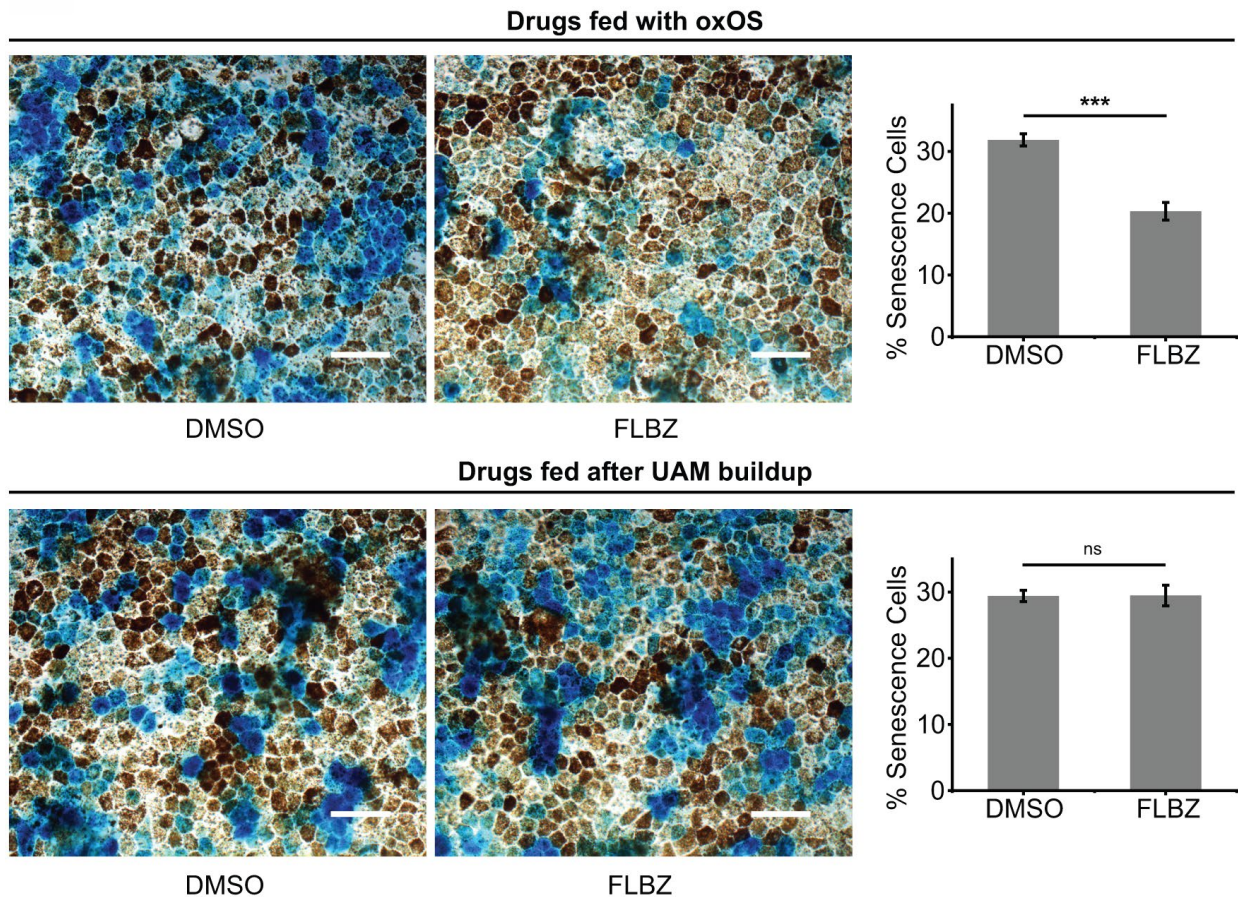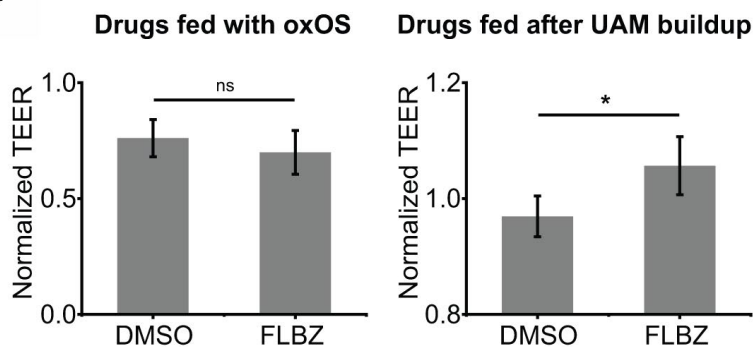


**Figure 5. FLBZ alleviates UAM-induced senescence and tight-junction disruption.** (**A**) (Top) FLBZ reduces senescence when fed concurrently with oxOS during UAM accumulation. (Bottom) FLBZ is unable to reverse established senescence induced by already accumulated UAM. FLBZ is fed daily together with oxOS for 20 days in a month (top) or after one month of 20 oxOS feedings to induce UAM buildup (bottom). DMSO as vehicle control. Senescence measured by β-galactosidase activity (blue). Scale bar: 50 μm. n=6. (**B**) While FLBZ does not reduce senescence when added to culture after UAM accumulation has already occurred, it does improve RPE cell health, as assessed by tight-junction integrity (TEER measured after 20 FLBZ feedings) (right). Left graph n=6, right graph n=12. *ns p > 0.05, *p < 0.05, ***p < 0.001.*

during OS ingestion is integral to coordinated phagocytosis [35, 36, 83], and activation of mTOR may be important for RPE survival under stress [84]. Given the deleterious effects of mTOR inhibition on RPE function in our primary culture system, we propose that the RPE requires a careful and time-dependent balance between mTOR activating and deactivating signals. Direct or immediate upstream modulation of mTOR may not, therefore, be therapeutically tractable.

In our model of RPE lipid handling (Figure 3A), the RPE ingests OS and lipoprotein particles as part of a daily lipid challenge. If OS are incompletely degraded, lipofuscin develops. Lipid that is fully degraded in the lysosome transits the endoplasmic reticulum and is packaged as lipid droplets. The lipid droplets that form after an RPE lipid challenge, however, dissipate quickly [85], in contrast to the longer-lived lipid droplets of adipocytes or hepatocytes. Further, the accumulation of bloated lipid vacuoles, a feature of many age-related diseases including atherosclerosis [86], cardiomyopathy [87], liver disease [86], and neurodegeneration [88, 89], is not a feature of RPE degeneration in macular degeneration. Thus, the RPE's large daily lipid load is actively degraded or secreted rather than stored long-term. Tipping the balance towards degradation may provide photoreceptors with KBs, an alternative fuel source, and decrease the amount of secreted lipoprotein that contributes to drusen formation. We found FLBZ altered the balance between degradation vs. secretion of lipid in our primary human RPE culture. By reducing lipid secretion, FLBZ has the potential to work synergistically in dry AMD with pharmacologic programs aimed at clearing already deposited lipid/drusen in Bruch's membrane [90, 91].

Current pharmaceutical approaches to lipofuscin reduction have focused on disrupting the retina's visual cycle, which produces the retinoids that contribute to lipofuscin accumulation. However, all visual cycle modulators have failed to date in human clinical trials, likely because the visual cycle is so integral to visual function [92]. Avoiding the disadvantages of visual cycle modulation, we found that autophagy induction both prevented and reduced the accumulation of lipofuscin-like material (i.e. UAM [72]) in primary RPE culture.

Autophagy may clear lipofuscin both by wholesale engulfment of granules in a process akin to autophagic engulfment of lysosomes [93] and by the natural upregulation of lysosomal capacity that accompanies autophagy induction [94, 95]. Alternatively, components of lipofuscin are known to trigger accumulation of cholesterol in the lysosome and reduce cholesterol concentration in cell membranes [96]. As phagosome transport to the lysosome depends on cholesterol-rich lipid rafts [97], alterations in cholesterol composition of cell membranes retards phagosome maturation, which may lead to further accumulation of lipofuscin. There is also evidence that lipofuscin-mediated accumulation of cholesterol in the lysosome indirectly triggers altered microtubule dynamics which, in turn, slows phagosome and autophagosome maturation [98], leading to further lipofuscin accumulation. Induction of autophagy may directly or indirectly alter the cholesterol dyshomeostasis triggered by lipofuscin, leading to improved degradation of OS components and decreased lipofuscin accumulation.

Under conditions where FLBZ prevented UAM accumulation, the drug also reduced senescence associated with UAM. Reduced senescence may decrease AMD-associated inflammation and neovascularization [99, 100], and drugs that specifically eliminate senescent cells are in early stage clinical development for macular degeneration [101, 102]. Consistent with reports on the difficulty of reversing senescence [103], FLBZ did not reduce senescence in cultures where UAM had already accumulated. Nevertheless, delaying FLBZ treatment until after UAM had fully accumulated still reduced UAM burden, compacted remaining UAM granules, and modestly improved cell health, as assessed by tight-junction integrity. We have previously shown that UAM granules slowly compact over 12 months in culture; the acceleration of this compaction process by autophagy may diminish reactivity and toxicity of lipofuscin-like granules [72]. Consistent with this hypothesis, lipofuscin granules in AMD are larger than those in normal age-related controls [104].

The mechanism of FLBZ's induction of autophagy is not fully understood. FLBZ is an agonist of ATG4, a cysteine protease necessary for cleaving the core autophagy protein LC3 into its active form [105]. Additionally, FLBZ appears to trigger depolymerization of dynamic microtubules (MT), while stabilizing acetylated MTs, a property unique among a range of other microtubule depolymerizing agents [12]. MT acetylation-triggered activation of the stress kinase JNK1 leads to Bcl-2 phosphorylation which, in turn, releases the upstream autophagy inducer Beclin1 from its inhibitory complex with Bcl-2 [12]. Interestingly, the single largest genetic risk factor for AMD, the HTRA1 locus, codes for a serine protease that, like FLBZ, has significant effects on MT stability [106]. Whether FLBZ's effects on autophagy and AMD histologic phenotypes described here depend on HTRA1 allele status is an area for further research.

Our study utilized primary human fetal RPE to model aspects of AMD. There are advantages and limitations with this model. Any culture model lacks the complete retinal ecosystem that contextualizes RPE function in animal models [107], and there is clear evidence for the involvement of the choroid, Bruch's, RPE, and photoreceptors in AMD pathogenesis. On the other hand, no AMD mouse model truly recapitulates drusen formation [3]. Certain models show Bruch's membrane thickening with potential cholesterol deposition but without the lipoprotein particle composition that dominates human drusen [3, 108]. Further, the entire lipoprotein system, fundamental for drusen formation in humans, is markedly different between mice and humans [41].

The fetal origin of our human RPE cultures is also conceptually at odds with modeling a disease whose overwhelming principal risk factor is age. Indeed, while lipofuscin formation and oxidative stress may play a role in AMD, human fetal RPE cultures demonstrate a robust resistance to lipofuscin accumulation [72] and oxidative stress, tolerating doses of the oxidant tert-butyl hydroperoxide that typically trigger significant damage and death in other RPE culture models [109–112]. On the other hand, our hfRPE cultures demonstrate deposition of apoE and hydroxyapatite drusen-like deposits in the Transwell, characteristic of AMD [113] (data not shown). Further, in contrast to primary adult human RPE cultures, hfRPE expresses the drusen-promoting apolipoprotein, apoE, at a high level that closely approximates apoE expression in human RPE *in vivo* (data not shown). To ensure our hfRPE cultures mimic *in vivo* RPE to the maximum extent possible, we grow hfRPE exclusively on Transwells for, on average, at least 3 months; only cultures with high TEER (usually > 500 $\Omega$*cm$^2$), high pigmentation, and uniformly cobblestone morphology are utilized for all experiments. We have previously shown, under these conditions, that the RPE maintains numerous characteristics of *in vivo* RPE [44].

In summary, we demonstrate that activation of autophagy through mechanisms that do not involve direct mTOR inhibition can mitigate the processes associated with extracellular drusen formation and intracellular lipofuscin accumulation without causing RPE toxicity. As drusen and lipofuscin are pathologic hallmarks of dry AMD, FLBZ is a promising candidate drug for this disease.

## MATERIALS AND METHODS

### Primary hfRPE and ARPE-19 culture

Human fetal eyes were obtained from Advanced Bioscience Resources (ABR, Alameda, California) and cultured according to previously published methods [44]. hfRPE was plated on Transwells at passage 1, and experiments were performed on hfRPE that was in culture, on average, for three months or more. All Transwell cultures demonstrate high pigmentation, cobblestone morphology, absence of any intertwined fibroblastic patches, and TEER of at least 375 $\Omega$*cm$^2$. Step-by-step directions for our hfRPE culture are available at https://medicine.umich.edu/sites/default/files/content/downloads/Human_RPE_Culture_Protocol.pdf. ARPE-19 cells were a gift from the Hjelmeland laboratory [114] and were cultured at passage 19 as previously described [72].

### Assaying for autophagy

Cell cultures were exposed to each putative autophagy inducer at a concentration indicated in Table 1 for 24 hours, lysed with 36μL of SDS sample buffer with β-mercaptoethanol, with 15μg of lysate loaded on a 4-15% gradient gel followed by transfer to a PVDF membrane. Blots were incubated with 1:1000 of LC3A/B antibody (Cell Signaling Technology, #4108s) overnight. Quantifying LC3-II/LC3-I ratio is a well-accepted method for determining autophagy induction [45], and this ratio was quantified in a non-saturated, linear range using the Azure c500 Imaging System (Azure Biosystems, Dublin, CA, USA) and a combination of AzureSpot and ImageJ software. The data in Figure 1A are not normalized, whereas the data in Figure 1B, 1C are normalized to the average combined value of the vehicle and drug groups within each experimental repeat. The extreme pigmentation of human fetal cultures, combined with the destruction of the LC3 epitope with melanin bleaching protocols, makes detection of LC3 by immunofluorescence in hfRPE difficult. We previously extensively tested a range of LC3 staining and puncta quantification protocols specifically adapted to pigmented hfRPE culture, and those were employed for this study [44]. At least five fields of view were randomly chosen, imaged with a Leica SP5 confocal microscope, and averaged together for each experimental replicate. Vendor and product number for autophagy inducers are listed in Supplementary Table 1. Phospho-ATG16L1 puncta immunofluorescence was performed on paraformaldehyde-fixed cells permeabilized with 50μg/mL of digitonin in PBS for 10 minutes at room temperature, followed by detergent-free conditions for the blocking, primary antibody, secondary antibody, and wash steps. The primary antibody (Abcam, #195242) was incubated in PBS + 1% BSA for 1 hour at room temperature at a dilution of 1:100. Autophagy flux in these experiments was blocked by incubating with 30 μM chloroquine (Sigma, #C6628) for 24 hours. Phospho-ATG16L1 puncta quantification was

determined by counting puncta number for each condition and then normalizing this number to the average puncta number across all fields of view for both the control and treatment condition. This is reported as the "Puncta Index" in Supplementary Figure 2.

## TEER and cell death assays

TEER and cell death were measured as outlined previously [72]. For cell death assays, maximum possible LDH release per Transwell was measured immediately after 2μL of the final experimental supernate was taken. The Transwell and supernate was then treated with 0.2% Triton X-100 for 15 minutes at 37° C followed by collection of an additional 2μL of supernate. Each experimental LDH release value was first normalized to total LDH release from the vehicle condition at that timepoint. All TEER and LDH release measurements were then additionally normalized to the vehicle group at the zero hour timepoint. Step-by-step directions for our measurement of TEER in hfRPE cultures on Transwells are available at https://medicine. umich.edu/sites/default/files/content/downloads/Measuring_Transepithelial_Electrical_Resistance.pdf.

## Phagocytosis assays

Phagocytosis assays using bovine outer segments was performed using the "pulse-only" method described previously [44]. Briefly, in order to capture the total consumption of OS introduced to RPE in a single Transwell, the apical chamber of each Transwell is incubated with 50μL of media containing $4 \times 10^6$ OS/mL and OS phagocytosis bridging ligands (recombinant human milk fat globule-EGF factor −8 (MFG-E8) (1.5μg/mL, Sino Biological, #10853-H08B) and purified Protein S (ProS) (4μg/mL, Enzyme Research Laboratories, #HPS)). In contrast to the pulse-chase method used in classical phagocytosis assays, OS were added ("pulse") but not washed off ("chase"). At various times after OS "pulse", we added 50μL T-PER lysis buffer (Thermo, #78510) plus complete protease inhibitor mini-tab (Thermo, #PIA32955) to the apical chamber. The collected lysate thus included both the RPE cell layer as well as the media above, containing the non-consumed OS. Once collected, the "supernatant + cell" lysate is subjected to SDS-PAGE and blotted with an N-terminally directed anti-rhodopsin antibody (1:5000 dilution, Encor BioTech, #MCA-B630). This assay provides an assessment of total OS consumption by staining for all non-consumed OS, whether those OS were in the media, bound on the RPE cell surface, or internalized but incompletely degraded. Rhodopsin values at the zero hour timepoint were used for normalization. Step-by-step directions for our OS isolation protocol are available at https://medicine.umich.edu/sites/default/files/content/downloads/Photoreceptor_Outer_Segment_Isolation.pdf.

## Measuring ApoE secretion and ketogenesis

After 24 hours of exposure to drugs, supernates were collected and subjected to western blotting for apoE detection and a fluorometric assay for β-HB detection (AAT Bioquest, #13831), as previously described [72]. Twelve microliters of apical and basolateral supernates for apoE were mixed with 4 μl of 4x sample buffer, run on SDS-PAGE, and blotted with antibody (Millipore, #AB947) at a dilution of 1:2000. ApoE secretion was assessed in the presence of our standard RPE culture media with 5% fetal bovine serum. Blotting of equivalent volumes of just RPE media with 5% fetal bovine serum demonstrates negligible amounts of apoE (data not shown), confirming that measured apoE in our experiments derive from RPE secretion and not bovine serum. ApoE and β-HB values were normalized to the average value of the vehicle and experimental group within each experimental repeat.

## Undigested autofluorescent material

UAM accumulation and quantification as well as assays on senescence were carried out as previously described [72]. UAM granule size was measured with Leica LAS X software using the length of the long axis of the granule ellipse.

## Statistical analysis

Means were compared using paired or unpaired two-tailed Student's t-test, as appropriate. All error bars represent standard error of the mean unless otherwise specified. For apoE secretion experiments, there were non-balanced technical replicates between experiments and within treatment groups of a given experimental repeat. To ensure our normalization scheme did not lead to bias, we confirmed the magnitude and significance of our findings using mixed effects modeling in R [115]. All results from the mixed effects analysis were concordant with values and significance reported in this study.

## Role of funding source

Funders had no role in the conception, execution, or publication of this study. J.M.L.M. had full access to all data in this study and claims final responsibility for the decision to submit for publication.

## Abbreviations

AMD: age-related macular degeneration; ApoE: apolipoprotein E; β-HB: beta-hydroxybutyrate; FDA:

(US) Federal Drug Administration; FLBZ: flubendazole; GSK: GSK 1059615 (dual mTOR and phosphoinositide-3-kinase inhibitor); hfRPE: human fetal retinal pigment epithelium (cultures); JNJ: JNJ-47965567 (P2X7 purinergic receptor antagonist); KB: ketone body; LC3: microtubule-associated protein 1A/1B-light chain 3; LDH: lactate dehydrogenase; mTOR: mammalian target of rapamycin; MT: microtubule; OS: (photoreceptor) outer segments; oxOS: photo-oxidized (photoreceptor) outer segments; RPE: retinal pigment epithelium; TEER: trans-epithelial electrical resistance; Torin: torin1 (mTOR inhibitor); UAM: undigestible autofluorescent material (lipofuscin-like material).

## AUTHOR CONTRIBUTIONS

## ACKNOWLEDGMENTS

## CONFLICTS OF INTEREST

## FUNDING

## REFERENCES

1. Handa JT, Cano M, Wang L, Datta S, Liu T. Lipids, oxidized lipids, oxidation-specific epitopes, and Age-related Macular Degeneration. Biochim Biophys Acta Mol Cell Biol Lipids. 2017; 1862:430–40.
   https://doi.org/10.1016/j.bbalip.2016.07.013
   PMID:27480216

2. Bowes Rickman C, Farsiu S, Toth CA, Klingeborn M. Dry age-related macular degeneration: mechanisms, therapeutic targets, and imaging. Invest Ophthalmol Vis Sci. 2013; 54:ORSF68–80.
   https://doi.org/10.1167/iovs.13-12757
   PMID:24335072

3. Curcio CA. Soft Drusen in Age-Related Macular Degeneration: Biology and Targeting Via the Oil Spill Strategies. Invest Ophthalmol Vis Sci. 2018; 59:AMD160–81.
   https://doi.org/10.1167/iovs.18-24882
   PMID:30357336

4. Boulton ME. Studying melanin and lipofuscin in RPE cell culture models. Exp Eye Res. 2014; 126:61–67.
   https://doi.org/10.1016/j.exer.2014.01.016
   PMID:25152361

5. Escrevente C, Falcão AS, Hall MJ. Formation of lipofuscin-like autofluorescent granules in the retinal pigment epithelium requires lysosome dysfunction. Biorxiv. 2021; 2021.02.23.432539.
   https://doi.org/10.1101/2021.02.23.432539

6. Nixon RA. The role of autophagy in neurodegenerative disease. Nat Med. 2013; 19:983–97.
   https://doi.org/10.1038/nm.3232
   PMID:23921753

7. Ward C, Martinez-Lopez N, Otten EG, Carroll B, Maetzel D, Singh R, Sarkar S, Korolchuk VI. Autophagy, lipophagy and lysosomal lipid storage disorders. Biochim Biophys Acta. 2016; 1861:269–84.
   https://doi.org/10.1016/j.bbalip.2016.01.006
   PMID:26778751

8. Adijanto J, Du J, Moffat C, Seifert EL, Hurle JB, Philp NJ. The retinal pigment epithelium utilizes fatty acids for ketogenesis. J Biol Chem. 2014; 289:20570–82.
   https://doi.org/10.1074/jbc.M114.565457
   PMID:24898254

9. Reyes-Reveles J, Dhingra A, Alexander D, Bragin A, Philp NJ, Boesze-Battaglia K. Phagocytosis-dependent ketogenesis in retinal pigment epithelium. J Biol Chem. 2017; 292:8038–47.
   https://doi.org/10.1074/jbc.M116.770784
   PMID:28302729

10. Boya P, Esteban-Martínez L, Serrano-Puebla A, Gómez-Sintes R, Villarejo-Zori B. Autophagy in the eye:

Development, degeneration, and aging. Prog Retin Eye Res. 2016; 55:206–45.
https://doi.org/10.1016/j.preteyeres.2016.08.001
PMID:27566190

11. Frost LS, Mitchell CH, Boesze-Battaglia K. Autophagy in the eye: implications for ocular cell health. Exp Eye Res. 2014; 124:56–66.
https://doi.org/10.1016/j.exer.2014.04.010
PMID:24810222

12. Chauhan S, Ahmed Z, Bradfute SB, Arko-Mensah J, Mandell MA, Won Choi S, Kimura T, Blanchet F, Waller A, Mudd MH, Jiang S, Sklar L, Timmins GS, et al. Pharmaceutical screen identifies novel target processes for activation of autophagy with a broad translational potential. Nat Commun. 2015; 6:8620.
https://doi.org/10.1038/ncomms9620 PMID:26503418

13. Tsvetkov AS, Miller J, Arrasate M, Wong JS, Pleiss MA, Finkbeiner S. A small-molecule scaffold induces autophagy in primary neurons and protects against toxicity in a Huntington disease model. Proc Natl Acad Sci USA. 2010; 107:16982–87.
https://doi.org/10.1073/pnas.1004498107
PMID:20833817

14. Lee JM, Wagner M, Xiao R, Kim KH, Feng D, Lazar MA, Moore DD. Nutrient-sensing nuclear receptors coordinate autophagy. Nature. 2014; 516:112–15.
https://doi.org/10.1038/nature13961 PMID:25383539

15. Miranda S, González-Rodríguez Á, García-Ramírez M, Revuelta-Cervantes J, Hernández C, Simó R, Valverde ÁM. Beneficial effects of fenofibrate in retinal pigment epithelium by the modulation of stress and survival signaling under diabetic conditions. J Cell Physiol. 2012; 227:2352–62.
https://doi.org/10.1002/jcp.22970 PMID:21826649

16. Debnath P, Govila V, Sharma M, Saini A, Pandey S. Glucometric assessment of gingival crevicular blood in diabetic and non-diabetic patients: a randomized clinical trial. J Oral Biol Craniofac Res. 2015; 5:2–6.
https://doi.org/10.1016/j.jobcr.2014.12.004
PMID:25853040

17. Lorenzi PL, Claerhout S, Mills GB, Weinstein JN. A curated census of autophagy-modulating proteins and small molecules: candidate targets for cancer therapy. Autophagy. 2014; 10:1316–26.
https://doi.org/10.4161/auto.28773
PMID:24906121

18. Iorio F, Isacchi A, di Bernardo D, Brunetti-Pierri N. Identification of small molecules enhancing autophagic function from drug network analysis. Autophagy. 2010; 6:1204–05.
https://doi.org/10.1073/pnas.1000138107
PMID:20930556

19. Kuramoto K, Wang N, Fan Y, Zhang W, Schoenen FJ, Frankowski KJ, Marugan J, Zhou Y, Huang S, He C. Autophagy activation by novel inducers prevents BECN2-mediated drug tolerance to cannabinoids. Autophagy. 2016; 12:1460–71.
https://doi.org/10.1080/15548627.2016.1187367
PMID:27305347

20. Hale CM, Cheng Q, Ortuno D, Huang M, Nojima D, Kassner PD, Wang S, Ollmann MM, Carlisle HJ. Identification of modulators of autophagic flux in an image-based high content siRNA screen. Autophagy. 2016; 12:713–26.
https://doi.org/10.1080/15548627.2016.1147669
PMID:27050463

21. Moruno Manchon JF, Uzor NE, Dabaghian Y, Furr-Stimming EE, Finkbeiner S, Tsvetkov AS. Cytoplasmic sphingosine-1-phosphate pathway modulates neuronal autophagy. Sci Rep. 2015; 5:15213.
https://doi.org/10.1038/srep15213 PMID:26477494

22. Williams A, Sarkar S, Cuddon P, Ttofi EK, Saiki S, Siddiqi FH, Jahreiss L, Fleming A, Pask D, Goldsmith P, O'Kane CJ, Floto RA, Rubinsztein DC. Novel targets for Huntington's disease in an mTOR-independent autophagy pathway. Nat Chem Biol. 2008; 4:295–305.
https://doi.org/10.1038/nchembio.79 PMID:18391949

23. Zhang L, Yu J, Pan H, Hu P, Hao Y, Cai W, Zhu H, Yu AD, Xie X, Ma D, Yuan J. Small molecule regulators of autophagy identified by an image-based high-throughput screen. Proc Natl Acad Sci USA. 2007; 104:19023–28.
https://doi.org/10.1073/pnas.0709695104
PMID:18024584

24. Tan CC, Yu JT, Tan MS, Jiang T, Zhu XC, Tan L. Autophagy in aging and neurodegenerative diseases: implications for pathogenesis and therapy. Neurobiol Aging. 2014; 35:941–57.
https://doi.org/10.1016/j.neurobiolaging.2013.11.019
PMID:24360503

25. Rubinsztein DC, Codogno P, Levine B. Autophagy modulation as a potential therapeutic target for diverse diseases. Nat Rev Drug Discov. 2012; 11:709–30.
https://doi.org/10.1038/nrd3802 PMID:22935804

26. Eisenberg T, Knauer H, Schauer A, Büttner S, Ruckenstuhl C, Carmona-Gutierrez D, Ring J, Schroeder S, Magnes C, Antonacci L, Fussi H, Deszcz L, Hartl R, et al. Induction of autophagy by spermidine promotes longevity. Nat Cell Biol. 2009; 11:1305–14.
https://doi.org/10.1038/ncb1975 PMID:19801973

27. Shibuya Y, Chang CC, Huang LH, Bryleva EY, Chang TY. Inhibiting ACAT1/SOAT1 in microglia stimulates autophagy-mediated lysosomal proteolysis and

increases Aβ1-42 clearance. J Neurosci. 2014; 34:14484–501.
https://doi.org/10.1523/JNEUROSCI.2567-14.2014
PMID:25339759

28. Vakifahmetoglu-Norberg H, Xia HG, Yuan J. Pharmacologic agents targeting autophagy. J Clin Invest. 2015; 125:5–13.
https://doi.org/10.1172/JCI73937 PMID:25654545

29. Muniz-Feliciano L, Doggett TA, Zhou Z, Ferguson TA. RUBCN/rubicon and EGFR regulate lysosomal degradative processes in the retinal pigment epithelium (RPE) of the eye. Autophagy. 2017; 13:2072–85.
https://doi.org/10.1080/15548627.2017.1380124
PMID:28933590

30. Kuo SY, Castoreno AB, Aldrich LN, Lassen KG, Goel G, Dančík V, Kuballa P, Latorre I, Conway KL, Sarkar S, Maetzel D, Jaenisch R, Clemons PA, et al. Small-molecule enhancers of autophagy modulate cellular disease phenotypes suggested by human genetics. Proc Natl Acad Sci USA. 2015; 112:E4281–87.
https://doi.org/10.1073/pnas.1512289112
PMID:26195741

31. Kaizuka T, Morishita H, Hama Y, Tsukamoto S, Matsui T, Toyota Y, Kodama A, Ishihara T, Mizushima T, Mizushima N. An Autophagic Flux Probe that Releases an Internal Control. Mol Cell. 2016; 64:835–49.
https://doi.org/10.1016/j.molcel.2016.09.037
PMID:27818143

32. Khan O, La Thangue NB. HDAC inhibitors in cancer biology: emerging mechanisms and clinical applications. Immunol Cell Biol. 2012; 90:85–94.
https://doi.org/10.1038/icb.2011.100 PMID:22124371

33. Guha S, Baltazar GC, Coffey EE, Tu LA, Lim JC, Beckel JM, Patel S, Eysteinsson T, Lu W, O'Brien-Jenkins A, Laties AM, Mitchell CH. Lysosomal alkalinization, lipid oxidation, and reduced phagosome clearance triggered by activation of the P2X7 receptor. FASEB J. 2013; 27:4500–09.
https://doi.org/10.1096/fj.13-236166 PMID:23964074

34. Takenouchi T, Nakai M, Iwamaru Y, Sugama S, Tsukimoto M, Fujita M, Wei J, Sekigawa A, Sato M, Kojima S, Kitani H, Hashimoto M. The activation of P2X7 receptor impairs lysosomal functions and stimulates the release of autophagolysosomes in microglial cells. J Immunol. 2009; 182:2051–62.
https://doi.org/10.4049/jimmunol.0802577
PMID:19201858

35. Chiang CK, Tworak A, Kevany BM, Xu B, Mayne J, Ning Z, Figeys D, Palczewski K. Quantitative phosphoproteomics reveals involvement of multiple signaling pathways in early phagocytosis by the retinal pigmented epithelium. J Biol Chem. 2017; 292:19826–39.
https://doi.org/10.1074/jbc.M117.812677
PMID:28978645

36. Yu B, Egbejimi A, Dharmat R, Xu P, Zhao Z, Long B, Miao H, Chen R, Wensel TG, Cai J, Chen Y. Phagocytosed photoreceptor outer segments activate mTORC1 in the retinal pigment epithelium. Sci Signal. 2018; 11:eaag3315.
https://doi.org/10.1126/scisignal.aag3315
PMID:29844054

37. Gensler G, Clemons TE, Domalpally A, Danis RP, Blodi B, Wells J 3rd, Rauser M, Hoskins J, Hubbard GB, Elman MJ, Fish GE, Brucker A, Margherio A, Chew EY. Treatment of Geographic Atrophy with Intravitreal Sirolimus: The Age-Related Eye Disease Study 2 Ancillary Study. Ophthalmol Retina. 2018; 2:441–50.
https://doi.org/10.1016/j.oret.2017.08.015
PMID:29806044

38. Ramkumar HL, Zhang J, Chan CC. Retinal ultrastructure of murine models of dry age-related macular degeneration (AMD). Prog Retin Eye Res. 2010; 29:169–90.
https://doi.org/10.1016/j.preteyeres.2010.02.002
PMID:20206286

39. Fletcher EL, Jobling AI, Greferath U, Mills SA, Waugh M, Ho T, de Iongh RU, Phipps JA, Vessey KA. Studying age-related macular degeneration using animal models. Optom Vis Sci. 2014; 91:878–86.
https://doi.org/10.1097/OPX.0000000000000322
PMID:24978866

40. Malek G, Busik J, Grant MB, Choudhary M. Models of retinal diseases and their applicability in drug discovery. Expert Opin Drug Discov. 2018; 13:359–77.
https://doi.org/10.1080/17460441.2018.1430136
PMID:29382242

41. Getz GS, Reardon CA. Use of Mouse Models in Atherosclerosis Research. Methods Mol Biol. 2015; 1339:1–16.
https://doi.org/10.1007/978-1-4939-2929-0_1
PMID:26445778

42. Lyssenko NN, Haider N, Picataggi A, Cipollari E, Jiao W, Phillips MC, Rader DJ, Chavali VR. Directional ABCA1-mediated cholesterol efflux and apoB-lipoprotein secretion in the retinal pigment epithelium. J Lipid Res. 2018; 59:1927–39.
https://doi.org/10.1194/jlr.M087361 PMID:30076206

43. Johnson LV, Forest DL, Banna CD, Radeke CM, Maloney MA, Hu J, Spencer CN, Walker AM, Tsie MS, Bok D, Radeke MJ, Anderson DH. Cell culture model that mimics drusen formation and triggers complement activation associated with age-related macular

degeneration. Proc Natl Acad Sci USA. 2011; 108:18277–82.
https://doi.org/10.1073/pnas.1109703108
PMID:21969589

44. Zhang Q, Presswalla F, Feathers K, Cao X, Hughes BA, Zacks DN, Thompson DA, Miller JM. A platform for assessing outer segment fate in primary human fetal RPE cultures. Exp Eye Res. 2019; 178:212–22.
https://doi.org/10.1016/j.exer.2018.10.008
PMID:30336126

45. Klionsky DJ, Abdelmohsen K, Abe A, Abedin MJ, Abeliovich H, Acevedo Arozena A, Adachi H, Adams CM, Adams PD, Adeli K, Adhihetty PJ, Adler SG, Agam G, et al. Guidelines for the use and interpretation of assays for monitoring autophagy (3rd edition). Autophagy. 2016; 12:1–222.
https://doi.org/10.1080/15548627.2015.1100356
PMID:26799652

46. Carnero A. Novel inhibitors of the PI3K family. Expert Opin Investig Drugs. 2009; 18:1265–77.
https://doi.org/10.1517/13543780903066798
PMID:19589091

47. Liu Q, Chang JW, Wang J, Kang SA, Thoreen CC, Markhard A, Hur W, Zhang J, Sim T, Sabatini DM, Gray NS. Discovery of 1-(4-(4-propionylpiperazin-1-yl)-3-(trifluoromethyl)phenyl)-9-(quinolin-3-yl)benzo[h][1, 6]naphthyridin-2(1H)-one as a highly potent, selective mammalian target of rapamycin (mTOR) inhibitor for the treatment of cancer. J Med Chem. 2010; 53:7146–55.
https://doi.org/10.1021/jm101144f
PMID:20860370

48. Cheong JK, Zhang F, Chua PJ, Bay BH, Thorburn A, Virshup DM. Casein kinase 1α-dependent feedback loop controls autophagy in RAS-driven cancers. J Clin Invest. 2015; 125:1401–18.
https://doi.org/10.1172/JCI78018 PMID:25798617

49. Lin CW, Chen YS, Lin CC, Chen YJ, Lo GH, Lee PH, Kuo PL, Dai CY, Huang JF, Chung WL, Yu ML. Amiodarone as an autophagy promoter reduces liver injury and enhances liver regeneration and survival in mice after partial hepatectomy. Sci Rep. 2015; 5:15807.
https://doi.org/10.1038/srep15807 PMID:26515640

50. Menzies FM, Garcia-Arencibia M, Imarisio S, O'Sullivan NC, Ricketts T, Kent BA, Rao MV, Lam W, Green-Thompson ZW, Nixon RA, Saksida LM, Bussey TJ, O'Kane CJ, Rubinsztein DC. Calpain inhibition mediates autophagy-dependent protection against polyglutamine toxicity. Cell Death Differ. 2015; 22:433–44.
https://doi.org/10.1038/cdd.2014.151 PMID:25257175

51. Min H, Xu M, Chen ZR, Zhou JD, Huang M, Zheng K, Zou XP. Bortezomib induces protective autophagy through AMP-activated protein kinase activation in cultured pancreatic and colorectal cancer cells. Cancer Chemother Pharmacol. 2014; 74:167–76.
https://doi.org/10.1007/s00280-014-2451-7
PMID:24842158

52. Renna M, Jimenez-Sanchez M, Sarkar S, Rubinsztein DC. Chemical inducers of autophagy that enhance the clearance of mutant proteins in neurodegenerative diseases. J Biol Chem. 2010; 285:11061–67.
https://doi.org/10.1074/jbc.R109.072181
PMID:20147746

53. Liu YL, Yang PM, Shun CT, Wu MS, Weng JR, Chen CC. Autophagy potentiates the anti-cancer effects of the histone deacetylase inhibitors in hepatocellular carcinoma. Autophagy. 2010; 6:1057–65.
https://doi.org/10.4161/auto.6.8.13365
PMID:20962572

54. Zhan Y, Gong K, Chen C, Wang H, Li W. P38 MAP kinase functions as a switch in MS-275-induced reactive oxygen species-dependent autophagy and apoptosis in human colon cancer cells. Free Radic Biol Med. 2012; 53:532–43.
https://doi.org/10.1016/j.freeradbiomed.2012.05.018
PMID:22634147

55. Schwartz EL, Ling YH, Zou Y, Piperdi B, Perez-Soler R. Abstract 850: Activation of autophagy by erlotinib protects NSCLC cells with wild-type EGFR from erlotinib cytotoxicity. Cancer Res. 2012 (Suppl); 72:850.
https://doi.org/10.1158/1538-7445.AM2012-850

56. Liu FT, Yang YJ, Wu JJ, Li S, Tang YL, Zhao J, Liu ZY, Xiao BG, Zuo J, Liu W, Wang J. Fasudil, a Rho kinase inhibitor, promotes the autophagic degradation of A53T α-synuclein by activating the JNK 1/Bcl-2/beclin 1 pathway. Brain Res. 2016; 1632:9–18.
https://doi.org/10.1016/j.brainres.2015.12.002
PMID:26683082

57. Zhang J, Cheng Y, Gu J, Wang S, Zhou S, Wang Y, Tan Y, Feng W, Fu Y, Mellen N, Cheng R, Ma J, Zhang C, et al. Fenofibrate increases cardiac autophagy via FGF21/SIRT1 and prevents fibrosis and inflammation in the hearts of Type 1 diabetic mice. Clin Sci (Lond). 2016; 130:625–41.
https://doi.org/10.1042/CS20150623
PMID:26795437

58. Barmada SJ, Serio A, Arjun A, Bilican B, Daub A, Ando DM, Tsvetkov A, Pleiss M, Li X, Peisach D, Shaw C, Chandran S, Finkbeiner S. Autophagy induction enhances TDP43 turnover and survival in neuronal ALS models. Nat Chem Biol. 2014; 10:677–85.
https://doi.org/10.1038/nchembio.1563
PMID:24974230

59. Yu HC, Lin CS, Tai WT, Liu CY, Shiau CW, Chen KF. Nilotinib induces autophagy in hepatocellular carcinoma through AMPK activation. J Biol Chem. 2013; 288:18249–59.
https://doi.org/10.1074/jbc.M112.446385
PMID:23677989

60. Tung YT, Wang BJ, Hu MK, Hsu WM, Lee H, Huang WP, Liao YF. Autophagy: a double-edged sword in Alzheimer's disease. J Biosci. 2012; 37:157–65.
https://doi.org/10.1007/s12038-011-9176-0
PMID:22357213

61. Perera ND, Sheean RK, Lau CL, Shin YS, Beart PM, Horne MK, Turner BJ. Rilmenidine promotes MTOR-independent autophagy in the mutant SOD1 mouse model of amyotrophic lateral sclerosis without slowing disease progression. Autophagy. 2018; 14:534–51.
https://doi.org/10.1080/15548627.2017.1385674
PMID:28980850

62. Luo R, Su LY, Li G, Yang J, Liu Q, Yang LX, Zhang DF, Zhou H, Xu M, Fan Y, Li J, Yao YG. Activation of PPARA-mediated autophagy reduces Alzheimer disease-like pathology and cognitive decline in a murine model. Autophagy. 2020; 16:52–69.
https://doi.org/10.1080/15548627.2019.1596488
PMID:30898012

63. To KK, Wu WK, Loong HH. PPARgamma agonists sensitize PTEN-deficient resistant lung cancer cells to EGFR tyrosine kinase inhibitors by inducing autophagy. Eur J Pharmacol. 2018; 823:19–26.
https://doi.org/10.1016/j.ejphar.2018.01.036
PMID:29378193

64. Xia D, Zhang YT, Xu GP, Yan WW, Pan XR, Tong JH. Sertraline exerts its antitumor functions through both apoptosis and autophagy pathways in acute myeloid leukemia cells. Leuk Lymphoma. 2017; 58:1–10.
https://doi.org/10.1080/10428194.2017.1287358
PMID:28278721

65. Tian W, Alsaadi R, Guo Z, Kalinina A, Carrier M, Tremblay ME, Lacoste B, Lagace D, Russell RC. An antibody for analysis of autophagy induction. Nat Methods. 2020; 17:232–39.
https://doi.org/10.1038/s41592-019-0661-y
PMID:31768061

66. Rizzolo LJ, Peng S, Luo Y, Xiao W. Integration of tight junctions and claudins with the barrier functions of the retinal pigment epithelium. Prog Retin Eye Res. 2011; 30:296–323.
https://doi.org/10.1016/j.preteyeres.2011.06.002
PMID:21704180

67. Rózanowski B, Burke JM, Boulton ME, Sarna T, Rózanowska M. Human RPE melanosomes protect from photosensitized and iron-mediated oxidation but become pro-oxidant in the presence of iron upon photodegradation. Invest Ophthalmol Vis Sci. 2008; 49:2838–47.
https://doi.org/10.1167/iovs.08-1700 PMID:18326697

68. Lobner D. Comparison of the LDH and MTT assays for quantifying cell death: validity for neuronal apoptosis? J Neurosci Methods. 2000; 96:147–52.
https://doi.org/10.1016/S0165-0270(99)00193-4
PMID:10720679

69. Cummings BS, Schnellmann RG. Measurement of cell death in mammalian cells. Curr Protoc Pharmacol. 2004. Chapter 12:Unit 12.8.
https://doi.org/10.1002/0471141755.ph1208s25
PMID:22294120

70. Mao Y, Finnemann SC. Analysis of photoreceptor outer segment phagocytosis by RPE cells in culture. Methods Mol Biol. 2013; 935:285–95.
https://doi.org/10.1007/978-1-62703-080-9_20
PMID:23150376

71. Pikuleva IA, Curcio CA. Cholesterol in the retina: the best is yet to come. Prog Retin Eye Res. 2014; 41:64–89.
https://doi.org/10.1016/j.preteyeres.2014.03.002
PMID:24704580

72. Zhang Q, Presswalla F, Calton M, Charniga C, Stern J, Temple S, Vollrath D, Zacks DN, Ali RR, Thompson DA, Miller JM. Highly Differentiated Human Fetal RPE Cultures Are Resistant to the Accumulation and Toxicity of Lipofuscin-Like Material. Invest Ophthalmol Vis Sci. 2019; 60:3468–79.
https://doi.org/10.1167/iovs.19-26690
PMID:31408109

73. Sun S, Cai B, Li Y, Su W, Zhao X, Gong B, Li Z, Zhang X, Wu Y, Chen C, Tsang SH, Yang J, Li X. HMGB1 and Caveolin-1 related to RPE cell senescence in age-related macular degeneration. Aging. 2019; 11:4323-37.
https://doi.org/10.18632/aging.102039
PMID: 31284269

74. Chen M, Xu H. Parainflammation, chronic inflammation, and age-related macular degeneration. J Leukoc Biol. 2015; 98:713–25.

https://doi.org/10.1189/jlb.3RI0615-239R
PMID:26292978

75. Sparrow JR. Bisretinoids of RPE lipofuscin: trigger for complement activation in age-related macular degeneration. Adv Exp Med Biol. 2010; 703:63–74.
https://doi.org/10.1007/978-1-4419-5635-4_5
PMID:20711707

76. Sparrow JR, Boulton M. RPE lipofuscin and its role in retinal pathobiology. Exp Eye Res. 2005; 80:595–606.

https://doi.org/10.1016/j.exer.2005.01.007
PMID:15862166

77. Zhang J, Bai Y, Huang L, Qi Y, Zhang Q, Li S, Wu Y, Li X. Protective effect of autophagy on human retinal pigment epithelial cells against lipofuscin fluorophore A2E: implications for age-related macular degeneration. Cell Death Dis. 2015; 6:e1972. https://doi.org/10.1038/cddis.2015.330 PMID:26561782

78. Mitter SK, Song C, Qi X, Mao H, Rao H, Akin D, Lewin A, Grant M, Dunn W Jr, Ding J, Bowes Rickman C, Boulton M. Dysregulated autophagy in the RPE is associated with increased susceptibility to oxidative stress and AMD. Autophagy. 2014; 10:1989–2005. https://doi.org/10.4161/auto.36184 PMID:25484094

79. Lakkaraju A, Umapathy A, Tan LX, Daniele L, Philp NJ, Boesze-Battaglia K, Williams DS. The cell biology of the retinal pigment epithelium. Prog Retin Eye Res. 2020. [Epub Ahead of Print]. https://doi.org/10.1016/j.preteyeres.2020.100846 PMID:32105772

80. Zhao C, Yasumura D, Li X, Matthes M, Lloyd M, Nielsen G, Ahern K, Snyder M, Bok D, Dunaief JL, LaVail MM, Vollrath D. mTOR-mediated dedifferentiation of the retinal pigment epithelium initiates photoreceptor degeneration in mice. J Clin Invest. 2011; 121:369–83. https://doi.org/10.1172/JCI44303 PMID:21135502

81. Chen Y, Wang J, Cai J, Sternberg P. Altered mTOR signaling in senescent retinal pigment epithelium. Invest Ophthalmol Vis Sci. 2010; 51:5314–19. https://doi.org/10.1167/iovs.10-5280 PMID:20445122

82. Yu B, Xu P, Zhao Z, Cai J, Sternberg P, Chen Y. Subcellular distribution and activity of mechanistic target of rapamycin in aged retinal pigment epithelium. Invest Ophthalmol Vis Sci. 2014; 55:8638–50. https://doi.org/10.1167/iovs.14-14758 PMID:25491300

83. Bulloj A, Duan W, Finnemann SC. PI 3-kinase independent role for AKT in F-actin regulation during outer segment phagocytosis by RPE cells. Exp Eye Res. 2013; 113:9–18. https://doi.org/10.1016/j.exer.2013.05.002 PMID:23669303

84. Halapin NA, Bazan NG. NPD1 induction of retinal pigment epithelial cell survival involves PI3K/Akt phosphorylation signaling. Neurochem Res. 2010; 35:1944–47. https://doi.org/10.1007/s11064-010-0351-8 PMID:21136150

85. Baker BN, Moriya M, Maude MB, Anderson RE, Williams TP. Oil droplets of the retinal epithelium of the rat. Exp Eye Res. 1986; 42:547–57. https://doi.org/10.1016/0014-4835(86)90045-X PMID:3720872

86. Krahmer N, Farese RV Jr, Walther TC. Balancing the fat: lipid droplets and human disease. EMBO Mol Med. 2013; 5:973–83. https://doi.org/10.1002/emmm.201100671 PMID:23740690

87. Goldberg IJ, Trent CM, Schulze PC. Lipid metabolism and toxicity in the heart. Cell Metab. 2012; 15:805–12. https://doi.org/10.1016/j.cmet.2012.04.006 PMID:22682221

88. Liu L, Zhang K, Sandoval H, Yamamoto S, Jaiswal M, Sanz E, Li Z, Hui J, Graham BH, Quintana A, Bellen HJ. Glial lipid droplets and ROS induced by mitochondrial defects promote neurodegeneration. Cell. 2015; 160:177–90. https://doi.org/10.1016/j.cell.2014.12.019 PMID:25594180

89. Di Paolo G, Kim TW. Linking lipids to Alzheimer's disease: cholesterol and beyond. Nat Rev Neurosci. 2011; 12:284–96. https://doi.org/10.1038/nrn3012 PMID:21448224

90. Rudolf M, Curcio CA, Schlötzer-Schrehardt U, Sefat AM, Tura A, Aherrahrou Z, Brinkmann M, Grisanti S, Miura Y, Ranjbar M. Apolipoprotein A-I Mimetic Peptide L-4F Removes Bruch's Membrane Lipids in Aged Nonhuman Primates. Invest Ophthalmol Vis Sci. 2019; 60:461–72. https://doi.org/10.1167/iovs.18-25786 PMID:30707219

91. Guymer RH, Wu Z, Hodgson LA, Caruso E, Brassington KH, Tindill N, Aung KZ, McGuinness MB, Fletcher EL, Chen FK, Chakravarthy U, Arnold JJ, Heriot WJ, et al, and Laser Intervention in Early Stages of Age-Related Macular Degeneration Study Group. Subthreshold Nanosecond Laser Intervention in Age-Related Macular Degeneration: The LEAD Randomized Controlled Clinical Trial. Ophthalmology. 2019; 126:829–38. https://doi.org/10.1016/j.ophtha.2018.09.015 PMID:30244144

92. Hussain RM, Gregori NZ, Ciulla TA, Lam BL. Pharmacotherapy of retinal disease with visual cycle modulators. Expert Opin Pharmacother. 2018; 19:471–81. https://doi.org/10.1080/14656566.2018.1448060 PMID:29542350

93. Hasegawa J, Maejima I, Iwamoto R, Yoshimori T. Selective autophagy: lysophagy. Methods. 2015; 75:128–32. https://doi.org/10.1016/j.ymeth.2014.12.014 PMID:25542097

94. Zhang XD, Qi L, Wu JC, Qin ZH. DRAM1 regulates autophagy flux through lysosomes. PLoS One. 2013; 8:e63245.
https://doi.org/10.1371/journal.pone.0063245
PMID:23696801

95. Yang M, Liu E, Tang L, Lei Y, Sun X, Hu J, Dong H, Yang SM, Gao M, Tang B. Emerging roles and regulation of MiT/TFE transcriptional factors. Cell Commun Signal. 2018; 16:31.
https://doi.org/10.1186/s12964-018-0242-1
PMID:29903018

96. Lakkaraju A, Finnemann SC, Rodriguez-Boulan E. The lipofuscin fluorophore A2E perturbs cholesterol metabolism in retinal pigment epithelial cells. Proc Natl Acad Sci USA. 2007; 104:11026–31.
https://doi.org/10.1073/pnas.0702504104
PMID:17578916

97. Rai A, Pathak D, Thakur S, Singh S, Dubey AK, Mallik R. Dynein Clusters into Lipid Microdomains on Phagosomes to Drive Rapid Transport toward Lysosomes. Cell. 2016; 164:722–34.
https://doi.org/10.1016/j.cell.2015.12.054
PMID:26853472

98. Toops KA, Tan LX, Jiang Z, Radu RA, Lakkaraju A. Cholesterol-mediated activation of acid sphingomyelinase disrupts autophagy in the retinal pigment epithelium. Mol Biol Cell. 2015; 26:1–14.
https://doi.org/10.1091/mbc.e14-05-1028
PMID:25378587

99. Kozlowski MR. RPE cell senescence: a key contributor to age-related macular degeneration. Med Hypotheses. 2012; 78:505–10.
https://doi.org/10.1016/j.mehy.2012.01.018
PMID:22296808

100. Zhu D, Deng X, Xu J, Hinton DR. What determines the switch between atrophic and neovascular forms of age related macular degeneration? - the role of BMP4 induced senescence. Aging (Albany NY). 2009; 1:740–45.
https://doi.org/10.18632/aging.100078
PMID:20157553

101. van Deursen JM. Senolytic therapies for healthy longevity. Science. 2019; 364:636–37.
https://doi.org/10.1126/science.aaw1299
PMID:31097655

102. Sreekumar PG, Hinton DR, Kannan R. The Emerging Role of Senescence in Ocular Disease. Oxid Med Cell Longev. 2020; 2020:2583601.
https://doi.org/10.1155/2020/2583601
PMID:32215170

103. Ohtani N. Deciphering the mechanism for induction of senescence-associated secretory phenotype (SASP) and its role in aging and cancer development. J Biochem. 2019. [Epub ahead of print].
https://doi.org/10.1093/jb/mvz055 PMID:31297533

104. Ach T, Tolstik E, Messinger JD, Zarubina AV, Heintzmann R, Curcio CA. Lipofuscin redistribution and loss accompanied by cytoskeletal stress in retinal pigment epithelium of eyes with age-related macular degeneration. Invest Ophthalmol Vis Sci. 2015; 56:3242–52.
https://doi.org/10.1167/iovs.14-16274
PMID:25758814

105. Zhang L, Guo M, Li J, Zheng Y, Zhang S, Xie T, Liu B. Systems biology-based discovery of a potential Atg4B agonist (Flubendazole) that induces autophagy in breast cancer. Mol Biosyst. 2015; 11:2860–66.
https://doi.org/10.1039/c5mb00466g
PMID:26299935

106. Melo E, Oertle P, Trepp C, Meistermann H, Burgoyne T, Sborgi L, Cabrera AC, Chen CY, Hoflack JC, Kam-Thong T, Schmucki R, Badi L, Flint N, et al. HtrA1 Mediated Intracellular Effects on Tubulin Using a Polarized RPE Disease Model. EBioMedicine. 2018; 27:258–74.
https://doi.org/10.1016/j.ebiom.2017.12.011
PMID:29269042

107. Kanow MA, Giarmarco MM, Jankowski CS, Tsantilas K, Engel AL, Du J, Linton JD, Farnsworth CC, Sloat SR, Rountree A, Sweet IR, Lindsay KJ, Parker ED, et al. Biochemical adaptations of the retina and retinal pigment epithelium support a metabolic ecosystem in the vertebrate eye. Elife. 2017; 6:e28899.
https://doi.org/10.7554/eLife.28899
PMID:28901286

108. van Leeuwen EM, Emri E, Merle BM, Colijn JM, Kersten E, Cougnard-Gregoire A, Dammeier S, Meester-Smoor M, Pool FM, de Jong EK, Delcourt C, Rodrigez-Bocanegra E, Biarnés M, et al. A new perspective on lipid research in age-related macular degeneration. Prog Retin Eye Res. 2018; 67:56–86.
https://doi.org/10.1016/j.preteyeres.2018.04.006
PMID:29729972

109. Tate DJ, Newsome DA. A novel zinc compound (zinc monocysteine) enhances the antioxidant capacity of human retinal pigment epithelial cells. Curr Eye Res. 2006; 31:675–83.
https://doi.org/10.1080/02713680600801024
PMID:16877276

110. Woo KI, Lee J. The effects of ascorbic acid on free radical injury in cultured retinal pigment epithelial cells. Korean J Ophthalmol. 1995; 9:19–25.
https://doi.org/10.3341/kjo.1995.9.1.19
PMID:7674549

111. Lee JJ, Ishihara K, Notomi S, Efstathiou NE, Ueta T, Maidana D, Chen X, Iesato Y, Caligiana A, Vavvas DG. Lysosome-associated membrane protein-2 deficiency increases the risk of reactive oxygen species-induced ferroptosis in retinal pigment epithelial cells. Biochem Biophys Res Commun. 2020; 521:414–19.
https://doi.org/10.1016/j.bbrc.2019.10.138
PMID:31672277

112. Miller JM, Zhang Q, Johnson MW. Regression of drusen or vitelliform material heralding geographic atrophy: correlation between clinical observations and basic science. Graefes Arch Clin Exp Ophthalmol. 2021. [Epub ahead of print].
https://doi.org/10.1007/s00417-021-05101-7
PMID:33547965

113. Pilgrim MG, Lengyel I, Lanzirotti A, Newville M, Fearn S, Emri E, Knowles JC, Messinger JD, Read RW, Guidry C, Curcio CA. Subretinal Pigment Epithelial Deposition of Drusen Components Including Hydroxyapatite in a Primary Cell Culture Model. Invest Ophthalmol Vis Sci. 2017; 58:708–19.
https://doi.org/10.1167/iovs.16-21060
PMID:28146236

114. Dunn KC, Aotaki-Keen AE, Putkey FR, Hjelmeland LM. ARPE-19, a human retinal pigment epithelial cell line with differentiated properties. Exp Eye Res. 1996; 62:155–69.
https://doi.org/10.1006/exer.1996.0020
PMID:8698076

115. Kuznetsova A, Brockhoff PB, Christensen RHB. lmerTest Package: Tests in Linear Mixed Effects Models. Journal of Statistical Software. 2017; 82:1–26.
https://doi.org/10.18637/jss.v082.i13
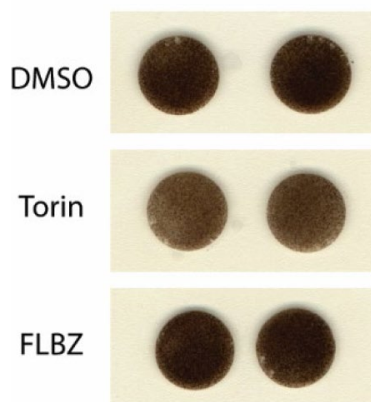
## Supplementary Figures
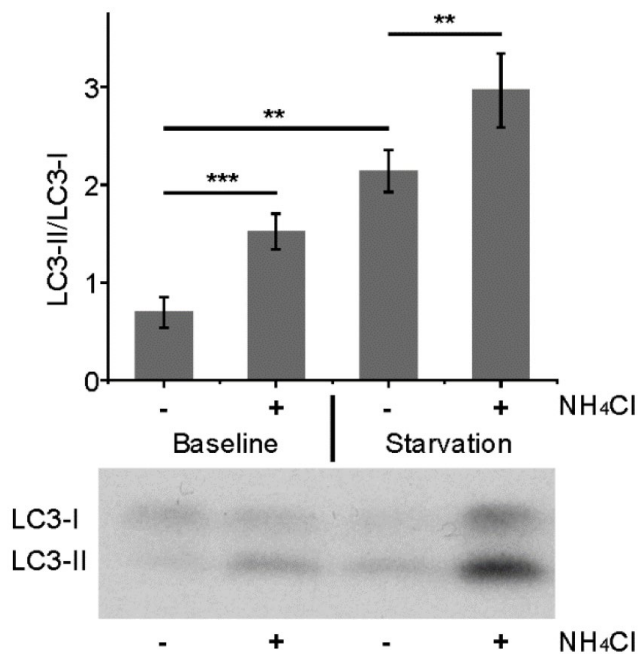


**Supplementary Figure 1. Serum and amino acid starvation induce autophagy flux in hfRPE.** Serum and amino acid starvation is induced by incubating hfRPE in Hank's Balanced Salt Solution for 6 hours, with normal media as control. The lysosomal alkalinizing agent NH4Cl (25 mM) was added 1.5 hours prior to harvest. In control wells, the increase in LC3-II/LC3-I ratio after blockade of autophagy flux by NH4Cl demonstrates that hfRPE has high baseline levels of constitutive autophagy. Amino acid and serum starvation with Hank's Balanced Salt Solution induces autophagy flux above baseline levels. n=6. **p < 0.01, ***p < 0.001.
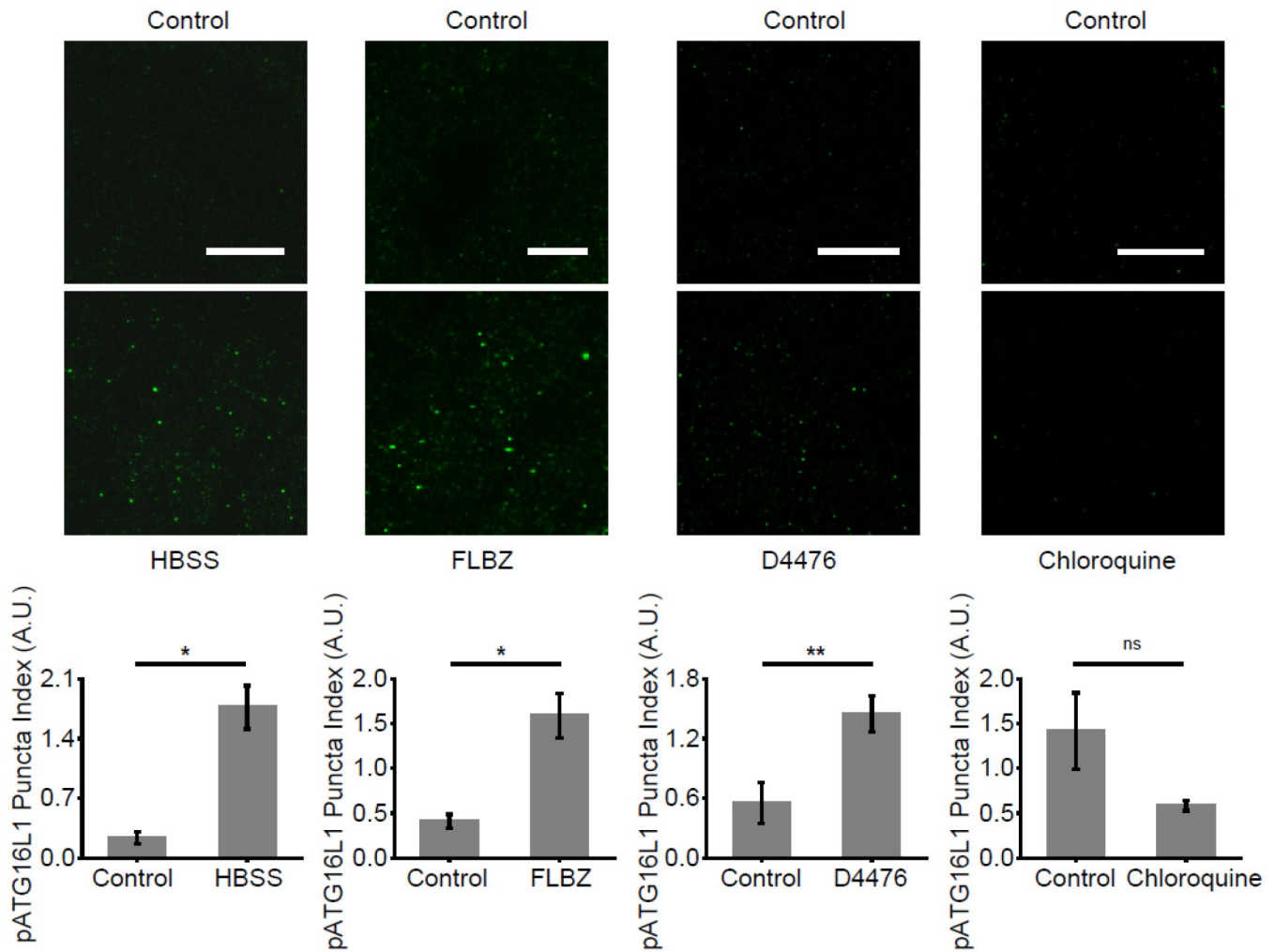
**Supplementary Figure 2. Phospho-ATG16L1 puncta formation confirms that serum and amino acid starvation, FLBZ, and D4476 stimulate autophagy flux.** Serum and amino acid starvation induced by incubating hfRPE in Hank's Balanced Salt Solution (HBSS) for 4 hours. Control cultures were incubated with normal media. FLBZ, D4476, and the lysosomal alkalinizing agent, chloroquine (30 μM), were incubated for 24 hours prior to immunostaining, with control wells containing the drug vehicle for FLBZ, D4476, or chloroquine. Phospho-ATG16L1 puncta staining demonstrates increased autophagy flux for serum and amino acid starvation, FLBZ, and D4476, and an expected decrease in flux with chloroquine treatment. Calculation of the puncta index is detailed in Methods. Scale bar: 10 μm. *ns p > 0.05, *p < 0.05, **p < 0.01.*
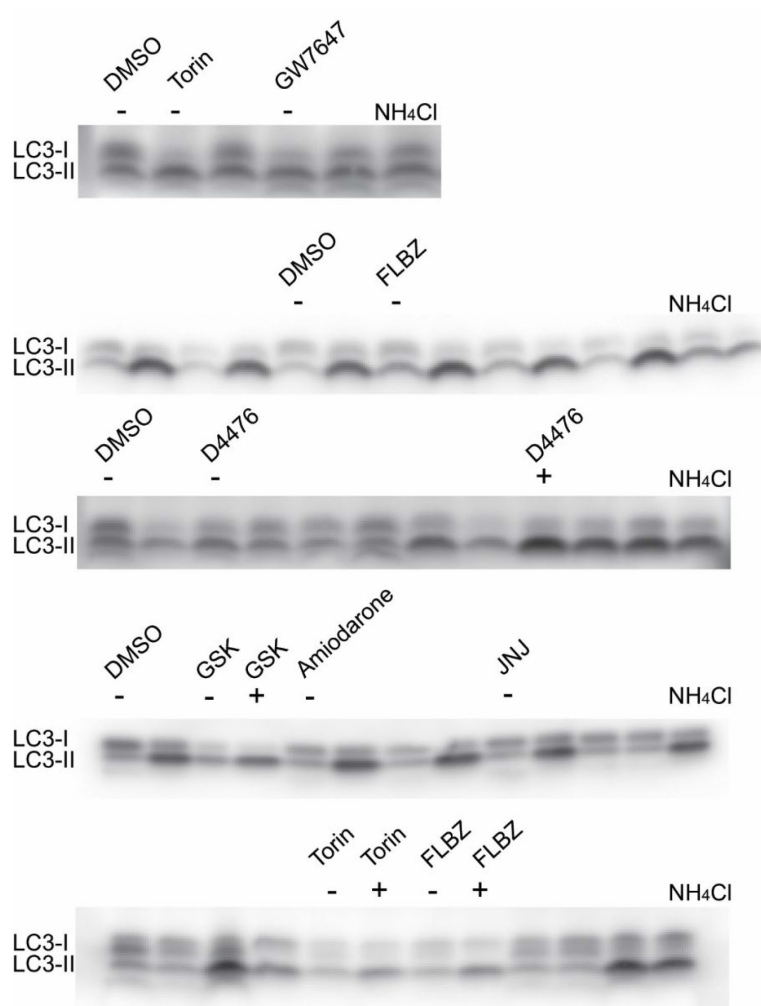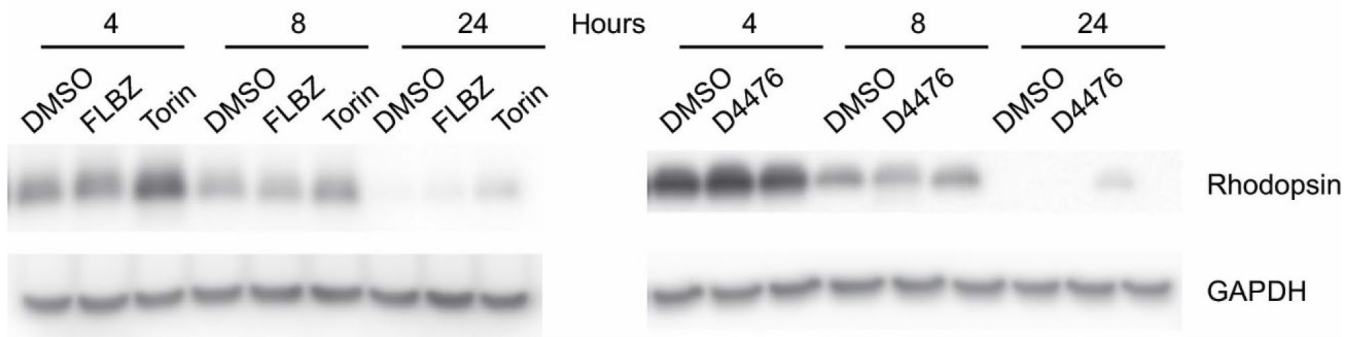
**Supplementary Figure 3. Uncropped western blots for Figure 1.** Symbols (+ or -) indicate presence or absence of NH$_4$Cl.



**Supplementary Figure 4. mTor inhibitor Torin1 reduces hfRPE pigmentation.** Whole mounted Transwells (in duplicate) are photographed. Daily feeding of oxOS and Torin together during UAM buildup resulted in reduced pigmentation (20 drug changes over 4 weeks). In contrast, an identical feeding protocol involving oxOS and FLBZ or oxOS and vehicle (DMSO) together during UAM buildup resulted in preserved pigmentation.
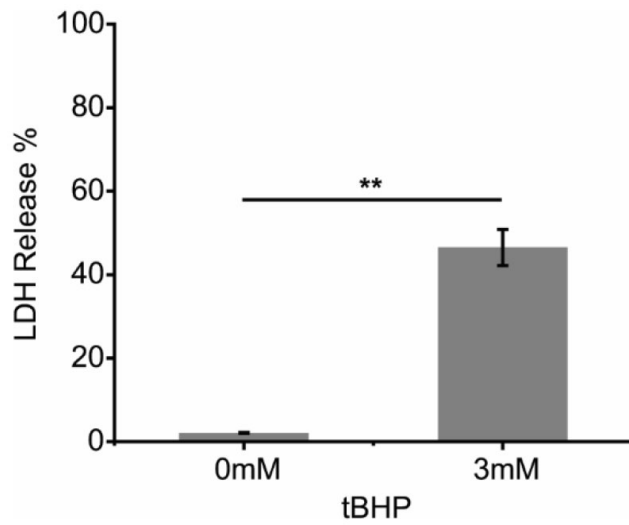
**Supplementary Figure 5. Lactate dehydrogenase (LDH) assay accurately assesses cell death, as determined by exposure to the oxidant tert-butyl hydroperoxide (tBHP).** Primary fetal RPE cultures were exposed to tBHP for 24 hours at a concentration known to cause partial but not complete cell death on the Transwell. There is a corresponding marked increase in LDH release. Data normalized to maximum possible LDH release as well as to the no tBHP condition.



**Supplementary Figure 6. Uncropped western blots for Figure 2.** The phagocytosis blots for GSK in Figure 2C are uncropped and therefore do not appear above.

## Supplementary Table

**Supplementary Table 1. Commercial sources for autophagy inducers in this study.**

| Name | Abbreviation | Company | Product number |
|---|---|---|---|
| GSK 1059615 | GSK | Sigma-Aldrich | SML0083 |
| Torin1 | Torin | ApexBio | A8312 |
| D4476 | | Cayman | 13305 |
| Flubendazole | FLBZ | Sigma-Aldrich | 34091 |
| Amiodarone | | Cayman | 15213 |
| GW7647 | | Cayman | 10008613 |
| JNJ-47965567 | JNJ | Cayman | 21895 |
| 2-Acetyl-5-tetrahydroxybutyl Imidazole | THI | Cayman | 13222 |
| Ac-Calpastatin | | Cayman | 16501 |
| AZ-10606120 | | Tocris | 3323 |
| Bortezomib | | Cayman | 10008822 |
| BRD5631 | | Broad Institute | MTA* |
| Carbamazepine | | Sigma-Aldrich | C4024 |
| Clonidine | | Sigma-Aldrich | C7897 |
| Entinostat | MS-275 | Cayman | 13284 |
| Erlotinib | | Cayman | 10483 |
| Fasudil | HA-1077 | Cayman | 10010559 |
| Fenofibrate | | Cayman | 10005368 |
| Fluphenazine | | MP Biomedical | ICN15370691 |
| K604 | | Otava LTD | 7070707145 |
| Loperamide | | Cayman | 14875 |
| Metformin | | Cayman | 13118 |
| ML246 | Metarrestin | AOBious | AOB1384 |
| Mocetinostat | | Cayman | 18287 |
| Nilotinib | | Cayman | 10010422 |
| Nilvadipine | | Sigma-Aldrich | SML0945 |
| Oxaprozin | | Cayman | 15476 |
| Rilmenidine | | Sigma-Aldrich | R134 |
| Saroglitazar | | Zydus-Cadila | MTA* |
| Sertraline | | Cayman | 14839 |
| Spermidine | | Sigma-Aldrich | S2626 |
| Trifluoperazine | | Sigma-Aldrich | T8516 |
| (±)-Verapamil | | Sigma-Aldrich | V4629 |

Direct mTOR inhibitors that induced autophagy in primary human fetal RPE cultures are highlighted in red. Compounds that do not directly inhibit mTOR but did induce autophagy in RPE cultures by both analysis of LC3 lipidation and LC3 puncta formation are highlighted in orange. Compounds that induced autophagy in RPE culture by only LC3 lipidation but not puncta formation are highlighted in green. All other compounds failed to induce LC3 lipidation in RPE cultures. *=Materials Transfer Agreement.